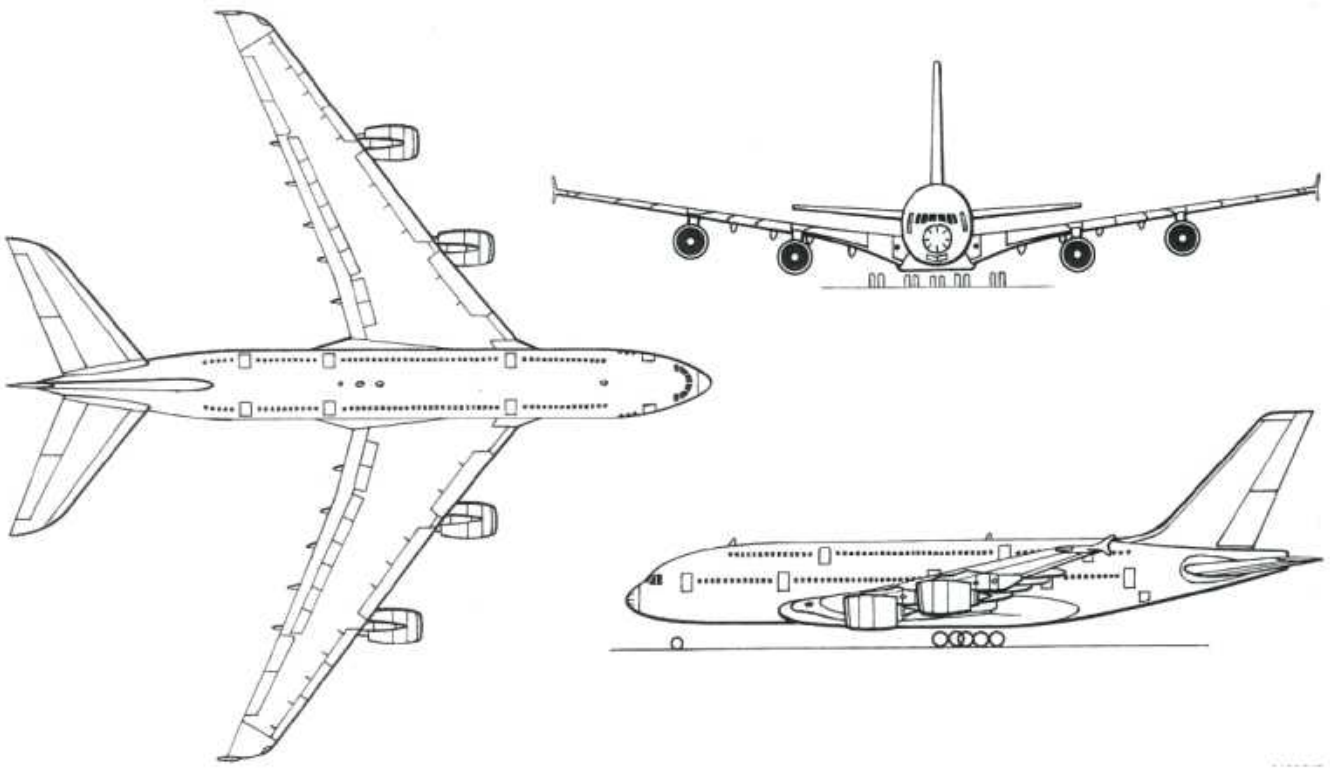

Airbus A380-800M, Image Source - SkyBrary Aviation

Flight Mechanics Project 2022-2023

Aircraft #8 Airbus A380-800M

Kanak Agarwal

Roll Number - 31
Registration Number - 210933058

Batch of 2021-2025
Manipal Institute of Technology
Bachelor of Technology in Aeronautical Engineering

June 13, 2024

Contents

1 Introduction

The following report outlines the methodology and the results of the performance analysis conducted on the Airbus A380- 800M as a part of the Flight Mechanics coursework for the academic year 2022-2023 at the Manipal Institute of Technology, Karnataka, India.

The performance analysis was conducted, and the results were plotted using MATLAB. LaTeXwas used to formulate the report. Once the results were plotted, they were analysed, and suitable conclusions were drawn from the respective polars.

While conducting the performance analysis of the aircraft, six aspects of the aircraft's performance were focused on. Namely, the drag polar, the flight envelope (V-h Plot), the aircraft's climb, turn, take-off and landing performance. All these analyses culminated into the Payload v/s Range trade-off study.

1.1 Preliminary Aircraft Data (A380-800M)

The following table elucidates the preliminary data used to conduct the performance analyses of the aircraft.

Parameter	**Value**
Take-off Weight (W_{TO})	6695 kN
Empty Weight (W_{Empty})	2725 kN
Payload Weight ($W_{Payload}$)	1480 kN
Fuel Weight (W_{Fuel})	2490 kN
Thrust per Engine (T)	350σ kN
Number of Engines	4
Thrust Specific Fuel Consumption (TSFC)	$47.5\sqrt{\theta}$ $^{kg}/_{hrkN}$
Wing Planform Area (S)	845 m^2
Wing Aspect Ratio (AR)	7.53
Oswald's Efficiency Factor (e)	0.965
Critical Mach Number (M_{crit})	0.895
Maximum permissible dynamic head (Aeroelastic limit or q_{max})	55 $^{kN}/_{m^2}$
Parasitic drag coefficient C_{D_0}	0.011
$C_{L_{max}}$ for climb segment of take-off	0.9 $C_{L_{max_{TO}}}$
C_L (ground effect)	0.12
$C_{L_{max}}$ (For Plain wing)	1.15
$\Delta C_{L_{max}}$ from partial HLD for take-off	1.15
$\Delta C_{L_{max}}$ from Full HLD for landing	1.85
$\Delta C_{D_{0\ Landing\ Gear}}$	0.0042
$\Delta C_{D_{0\ Flap}}$	0.0034
Rolling Coefficient μ	0.02
Extra Fuel tank Capacity	30% of W_{Fuel}
Cruise Altitude	12 km

Table 1: Preliminary Data

2 Drag Polar

2.1 Preliminary Calculations

The drag polar and, by extension, the analysis of the aircraft's drag was carried out for three take-off weights and six altitudes. The weights considered for the analysis were 0.9 W_{TO}, 0.8 W_{TO} and 0.6 W_{TO}.

The altitudes at which the drag was estimated were 0.5 km, 3 km, 5.5 km, 8.5 km, 10.5 km and 11.5 km. The V_{stall} and the V_{crit} boundaries were marked to signify the flight envelope limits on each polar. Further, the minimum drag D_{min} and their respective velocities $V_{D_{min}}$ were also calculated.

The total drag coefficient is written as,

$$C_D = C_{D_0} + C_{D_i} + C_{D_{wave}} \tag{1}$$

where C_{D_0} is the parasitic drag coefficient, C_{D_i} is the induced drag coefficient and $C_{D_{wave}}$ is the wave drag coefficient. The term $C_{D_{wave}}$ is zero for subsonic and transonic flight. Hence it is neglected, leading to the equation,

$$C_D = C_{D_0} + C_{D_i} \tag{2}$$

Substituting the value for C_{D_i} we get,

$$C_D = C_{D_0} + kC_L^2 \tag{3}$$

From this relation, we can obtain drag for level flight,

$$D = \left(C_{D_0} + kC_L^2\right)\left[{}^1\!/\!_2\rho V^2 S\right] \tag{4}$$

However, for level flight,

$$C_L = \frac{W}{{}^1\!/\!_2\rho V^2 S} \tag{5}$$

Substituting for C_{D_0} in equation 4 we get,

$$D = AV^2 + {}^B\!/\!_{V^2} \tag{6}$$

where A = ${}^{C_{D_0}\rho S}\!/\!_2$ and B = ${}^{2kW^2}\!/\!_{\rho S}$. The flight speed for minimum drag $V_{D_{min}}$ was obtained from the plot. The corresponding minimum drag D_{min} was identified from the respective drag polars. The flight envelope was defined by the region of the plot between the V_{stall} and the V_{crit} values for each corresponding curve.

The stall velocity V_{stall} was calculated using the relation,

$$V_{stall} = \sqrt{\frac{2W_{TO}}{\rho S C_{L_{max}}}} \tag{7}$$

The critical velocity (V_{crit}) was calculated from the initial value at sea level by varying the speed of sound according to the altitude.

2.2 Drag Polar for 0.9 W_{TO}

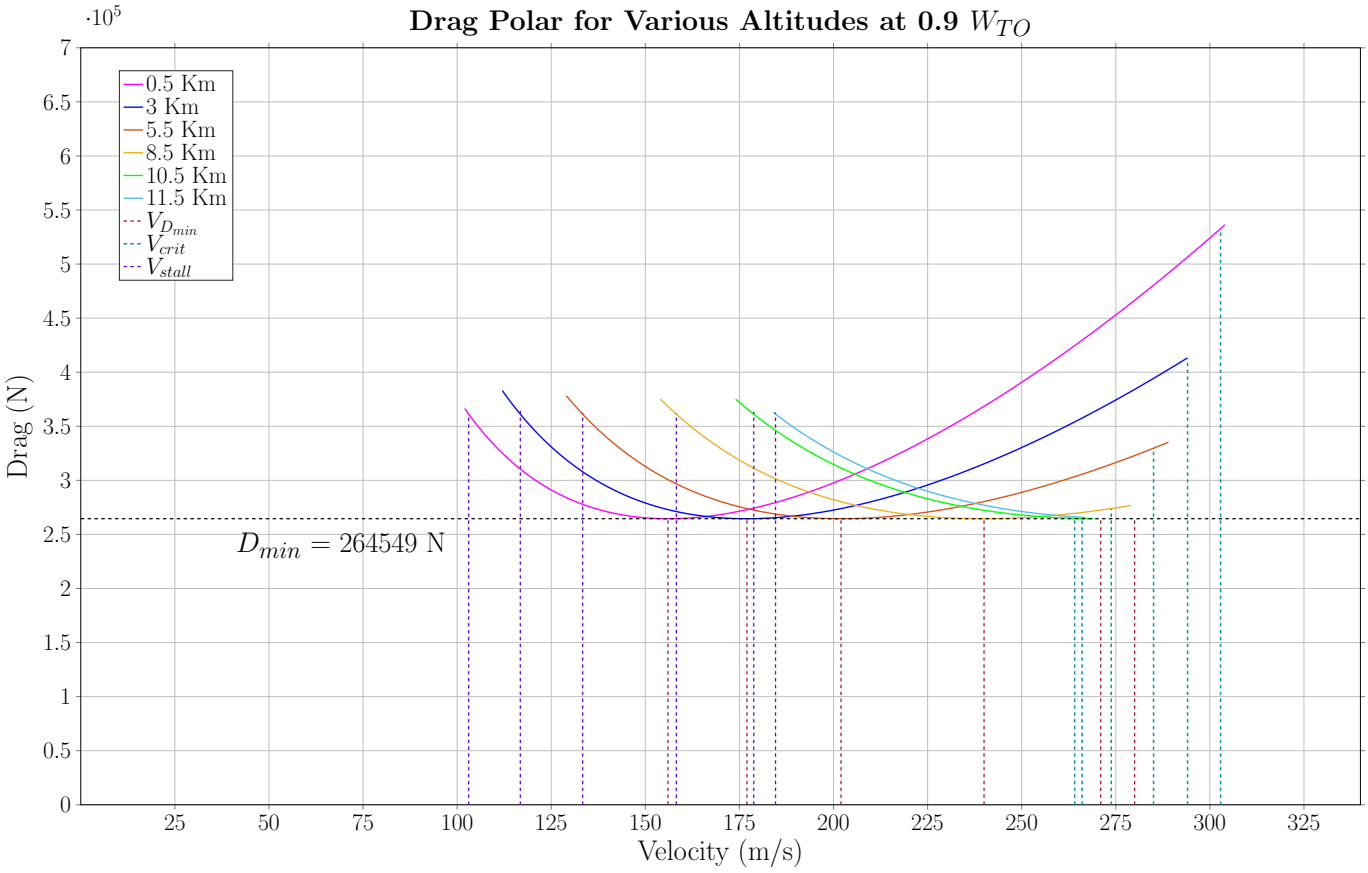

Parameter	Value
Take-off Weight (W_{TO})	6025.5 kN
V_{stall} at 0.5 km	103.06 m/s
V_{stall} at 3 km	116.78 m/s
V_{stall} at 5.5 km	133.36 m/s
V_{stall} at 8.5 km	158.24 m/s
V_{stall} at 10.5 km	178.81 m/s
V_{stall} at 11.5 km	184.60 m/s
$V_{D_{min}}$ at 0.5 km	156 m/s
$V_{D_{min}}$ at 3 km	177 m/s
$V_{D_{min}}$ at 5.5 km	202 m/s

Parameter	Value
Take-off Weight (W_{TO})	6025.5 kN
$V_{D_{min}}$ at 8.5 km	240 m/s
$V_{D_{min}}$ at 10.5 km	271 m/s
$V_{D_{min}}$ at 11.5 km	280 m/s
V_{crit} at 0.5 km	302.84 m/s
V_{crit} at 3 km	294.07 m/s
V_{crit} at 5.5 km	285.04 m/s
V_{crit} at 8.5 km	273.80 m/s
V_{crit} at 10.5 km	266.05 m/s
V_{crit} at 11.5 km	264.07 m/s

Table 2: Data for 0.9 W_{TO}

2.3 Drag Polar for 0.8 W_{TO}

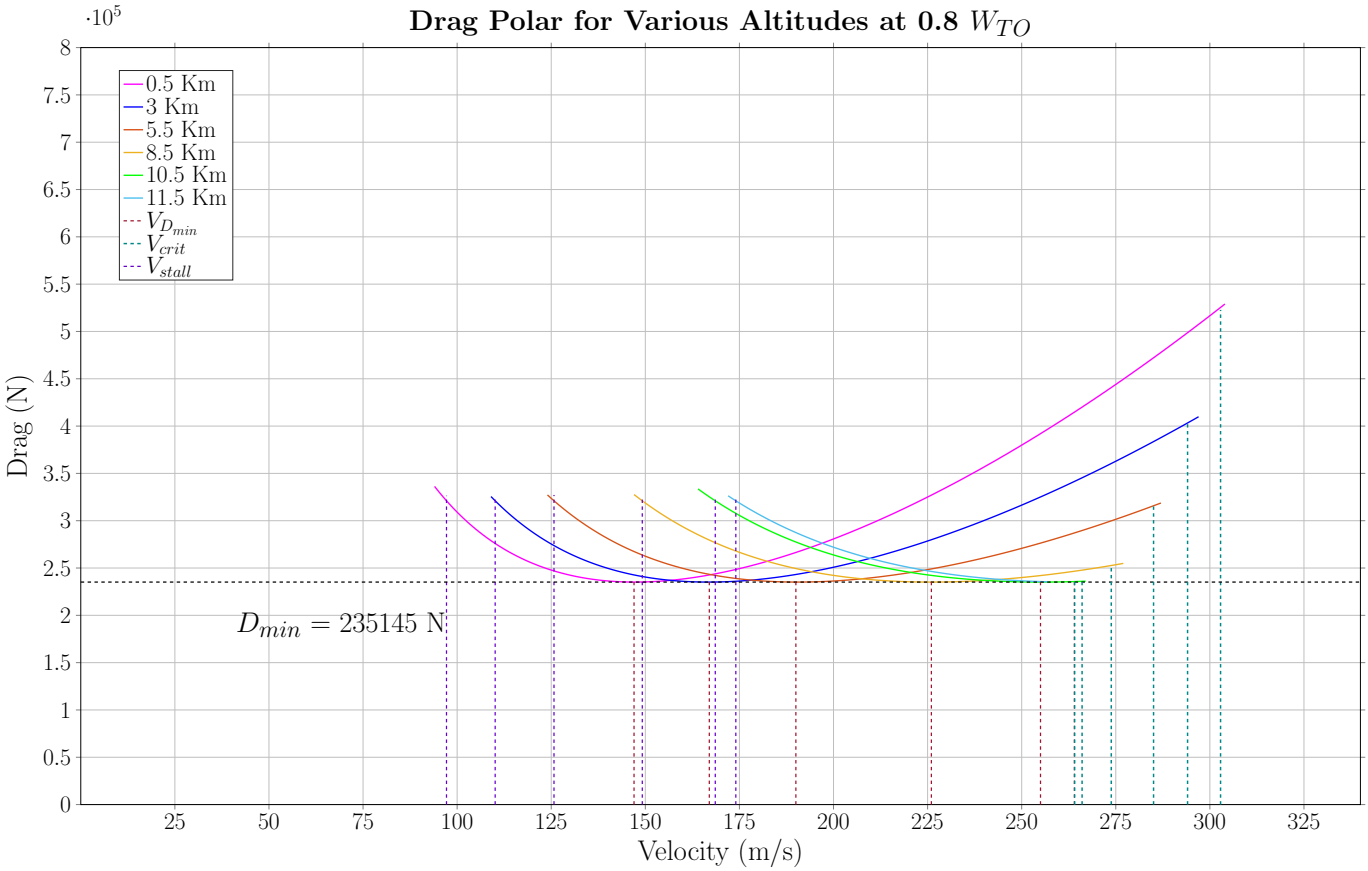

Parameter	Value
Take-off Weight (W_{TO})	5356 kN
V_{stall} at 0.5 km	97.17 m/s
V_{stall} at 3 km	110.10 m/s
V_{stall} at 5.5 km	125.73 m/s
V_{stall} at 8.5 km	149.19 m/s
V_{stall} at 10.5 km	168.58 m/s
V_{stall} at 11.5 km	174.04 m/s
$V_{D_{min}}$ at 0.5 km	147 m/s
$V_{D_{min}}$ at 3 km	167 m/s
$V_{D_{min}}$ at 5.5 km	190 m/s

Parameter	Value
Take-off Weight (W_{TO})	5356 kN
$V_{D_{min}}$ at 8.5 km	226 m/s
$V_{D_{min}}$ at 10.5 km	255 m/s
$V_{D_{min}}$ at 11.5 km	264 m/s
V_{crit} at 0.5 km	302.84 m/s
V_{crit} at 3 km	294.07 m/s
V_{crit} at 5.5 km	285.04 m/s
V_{crit} at 8.5 km	273.80 m/s
V_{crit} at 10.5 km	266.05 m/s
V_{crit} at 11.5 km	264.07 m/s

Table 3: Data for 0.8 W_{TO}

2.4 Drag Polar for 0.6 W_{TO}

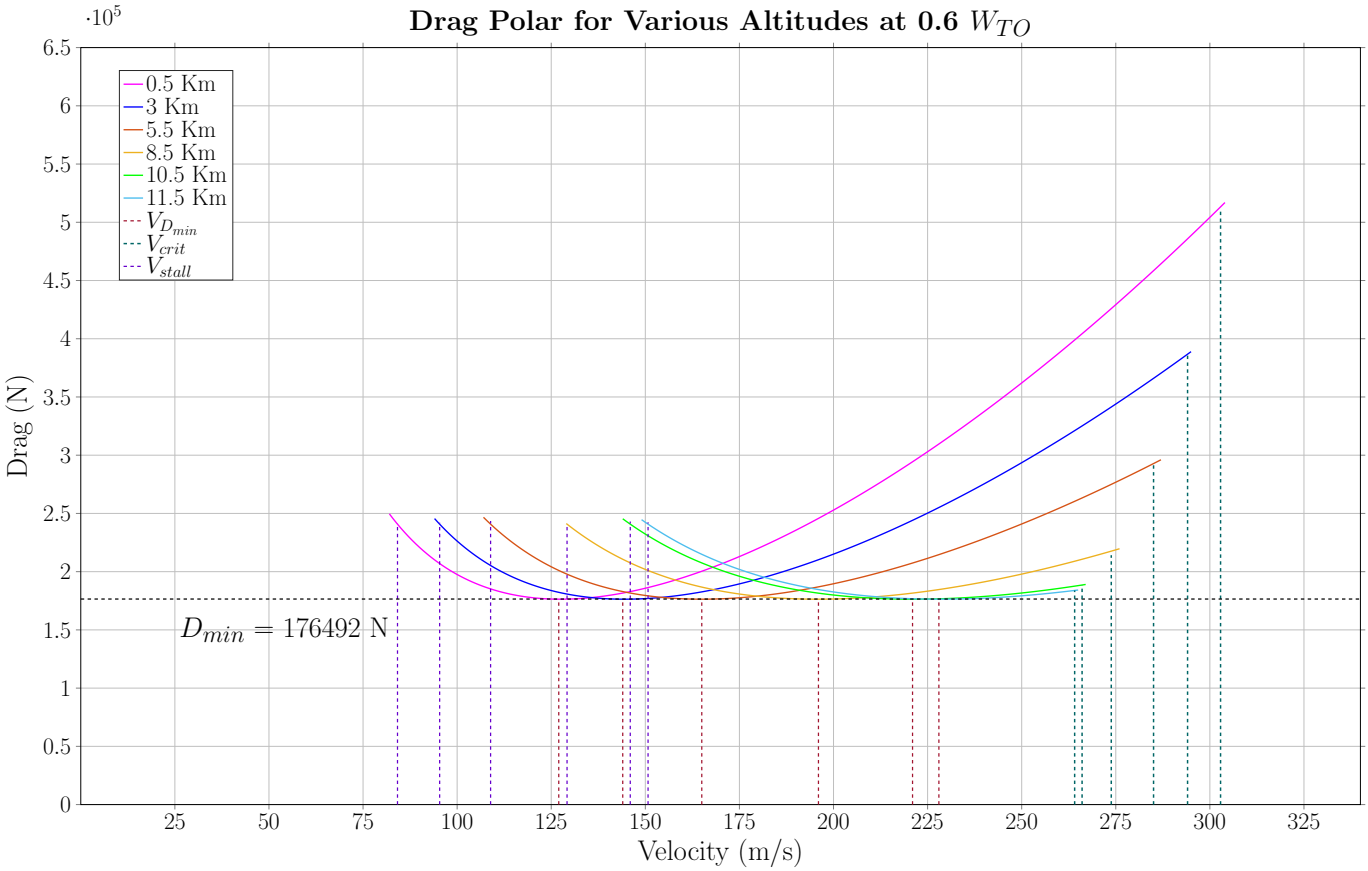

Parameter	Value
Take-off Weight (W_{TO})	4017 kN
V_{stall} at 0.5 km	84.15 m/s
V_{stall} at 3 km	95.35 m/s
V_{stall} at 5.5 km	108.88 m/s
V_{stall} at 8.5 km	129.20 m/s
V_{stall} at 10.5 km	145.99 m/s
V_{stall} at 11.5 km	150.72 m/s
$V_{D_{min}}$ at 0.5 km	127 m/s
$V_{D_{min}}$ at 3 km	144 m/s
$V_{D_{min}}$ at 5.5 km	165 m/s

Parameter	Value
Take-off Weight (W_{TO})	4017 kN
$V_{D_{min}}$ at 8.5 km	196 m/s
$V_{D_{min}}$ at 10.5 km	221 m/s
$V_{D_{min}}$ at 11.5 km	228 m/s
V_{crit} at 0.5 km	302.84 m/s
V_{crit} at 3 km	294.07 m/s
V_{crit} at 5.5 km	285.04 m/s
V_{crit} at 8.5 km	273.80 m/s
V_{crit} at 10.5 km	266.05 m/s
V_{crit} at 11.5 km	264.07 m/s

Table 4: Data for 0.6 W_{TO}

2.5 Drag Polar for 0.5 km

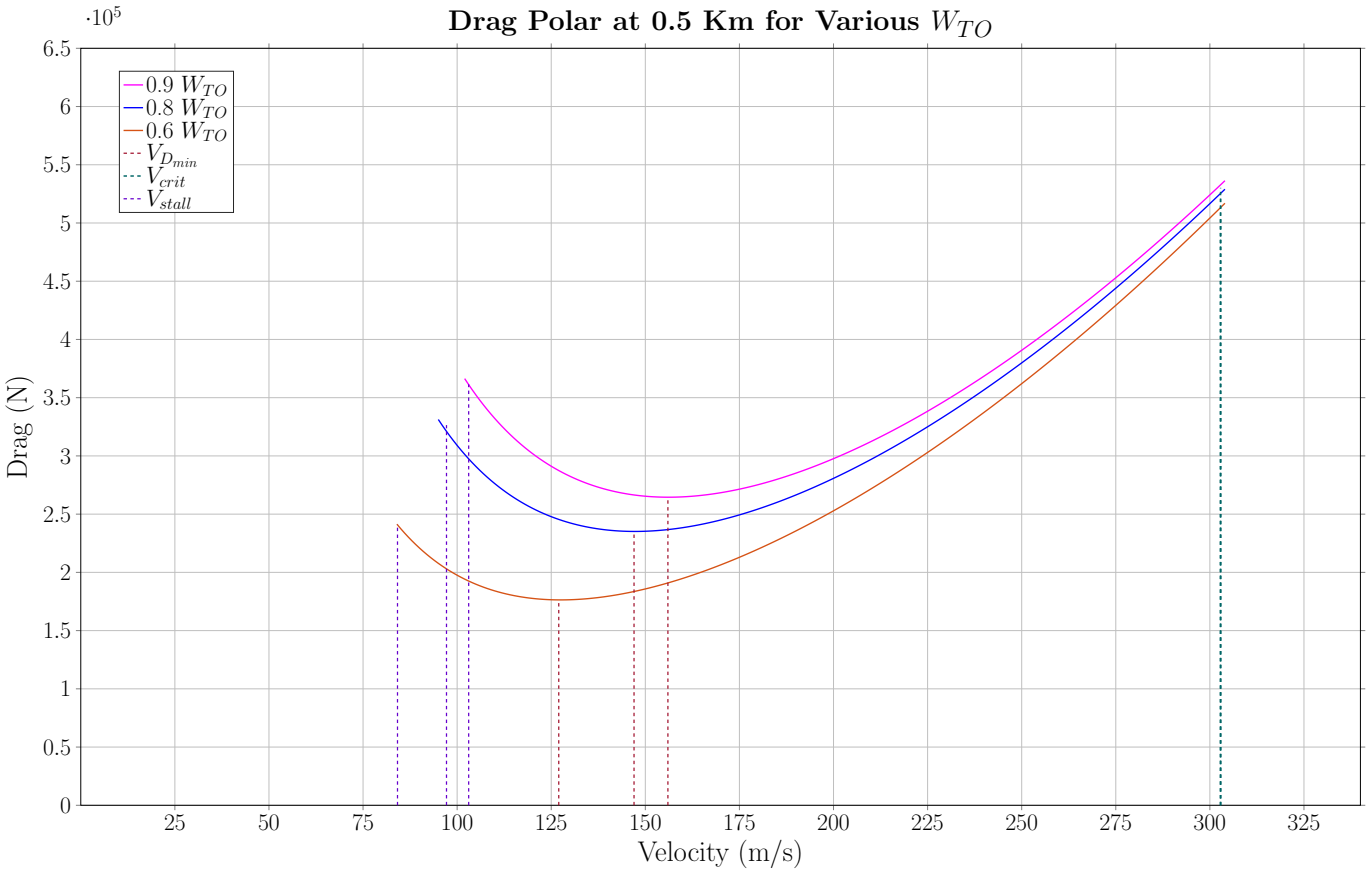

Parameter	Value
Altitude	0.5 km
V_{stall} at 0.9 W_{TO}	103.06 m/s
V_{stall} at 0.8 W_{TO}	97.17 m/s
V_{stall} at 0.6 W_{TO}	84.15 m/s
$V_{D_{min}}$ at 0.9 W_{TO}	156 m/s
$V_{D_{min}}$ at 0.8 W_{TO}	147 m/s
$V_{D_{min}}$ at 0.6 W_{TO}	127 m/s
V_{crit} at 0.9 W_{TO}	302.84 m/s
V_{crit} at 0.8 W_{TO}	302.84 m/s
V_{crit} at 0.6 W_{TO}	302.84 m/s

Table 5: Data for 0.5 km

2.6 Drag Polar for 3 km

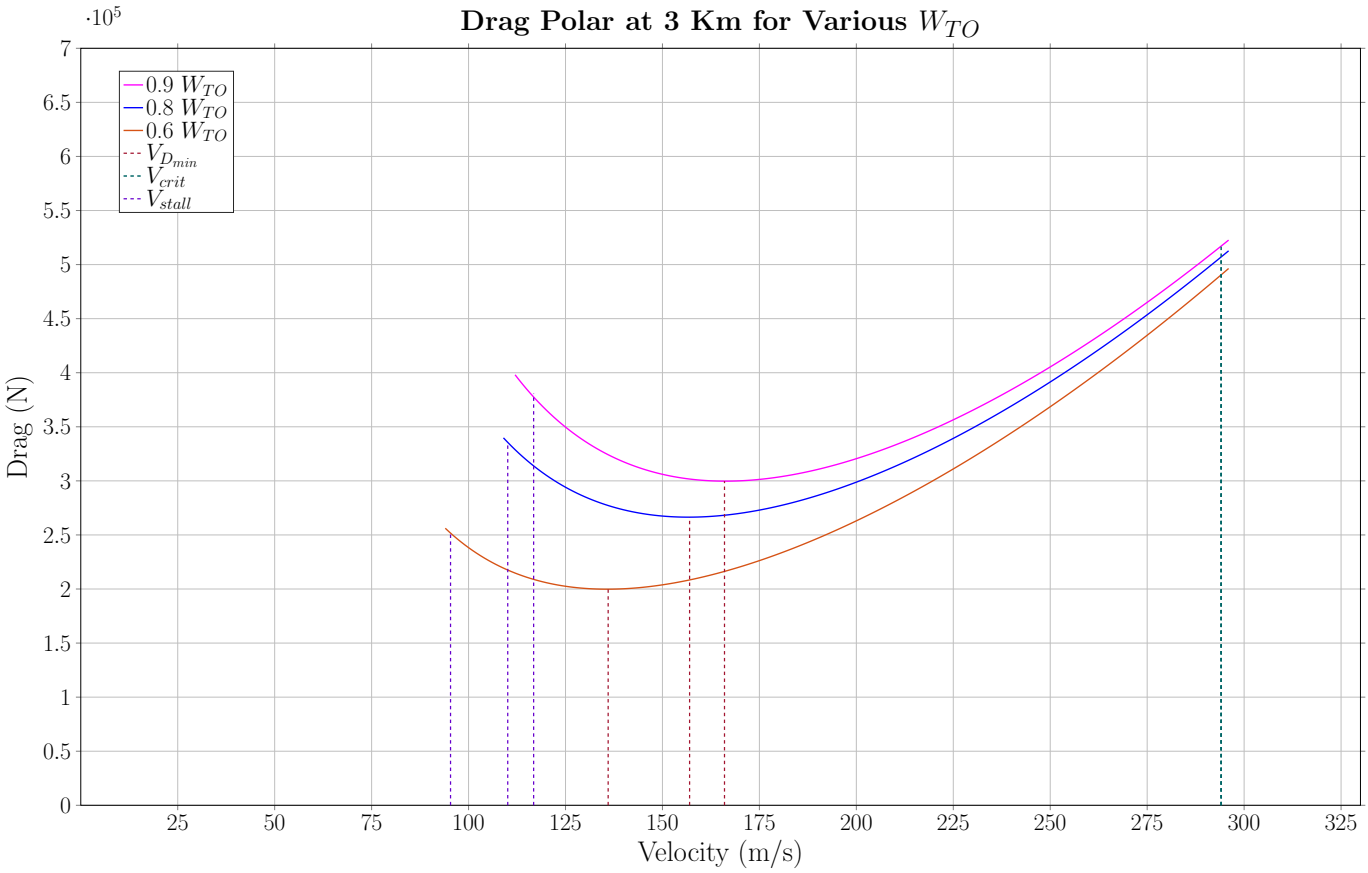

Parameter	Value
Altitude	3 km
V_{stall} at 0.9 W_{TO}	116.78 m/s
V_{stall} at 0.8 W_{TO}	97.17 m/s
V_{stall} at 0.6 W_{TO}	84.15 m/s
$V_{D_{min}}$ at 0.9 W_{TO}	156 m/s
$V_{D_{min}}$ at 0.8 W_{TO}	147 m/s
$V_{D_{min}}$ at 0.6 W_{TO}	127 m/s
V_{crit} at 0.9 W_{TO}	294.07 m/s
V_{crit} at 0.8 W_{TO}	294.07 m/s
V_{crit} at 0.6 W_{TO}	294.07 m/s

Table 6: Data for 3 km

2.7 Drag Polar for 5.5 km

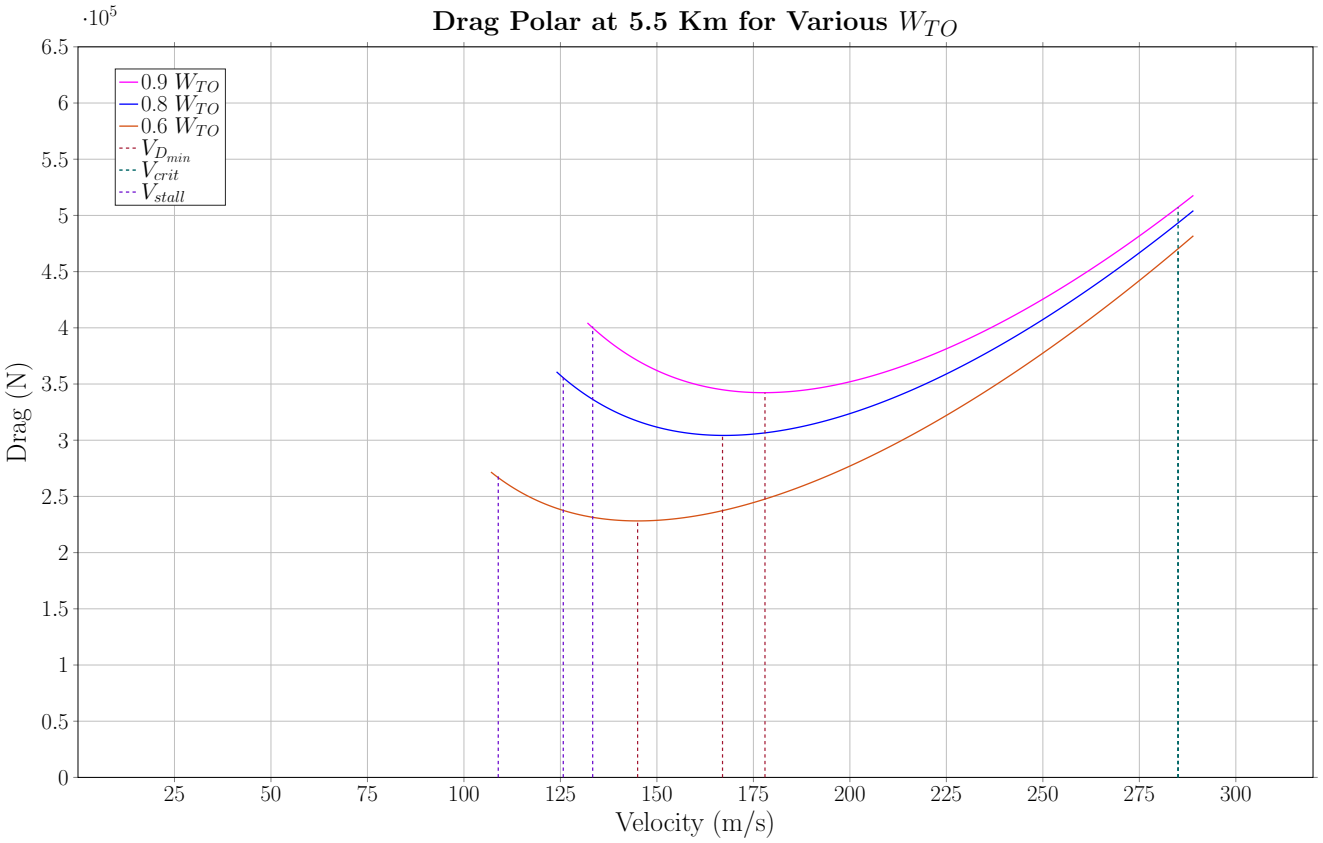

Parameter	Value
Altitude	0.5 km
V_{stall} at 0.9 W_{TO}	103.06 m/s
V_{stall} at 0.8 W_{TO}	97.17 m/s
V_{stall} at 0.6 W_{TO}	84.15 m/s
$V_{D_{min}}$ at 0.9 W_{TO}	156 m/s
$V_{D_{min}}$ at 0.8 W_{TO}	147 m/s
$V_{D_{min}}$ at 0.6 W_{TO}	127 m/s
V_{crit} at 0.9 W_{TO}	285.04 m/s
V_{crit} at 0.8 W_{TO}	285.04 m/s
V_{crit} at 0.6 W_{TO}	285.04 m/s

Table 7: Data for 5.5 km

2.8 Drag Polar for 8.5 km

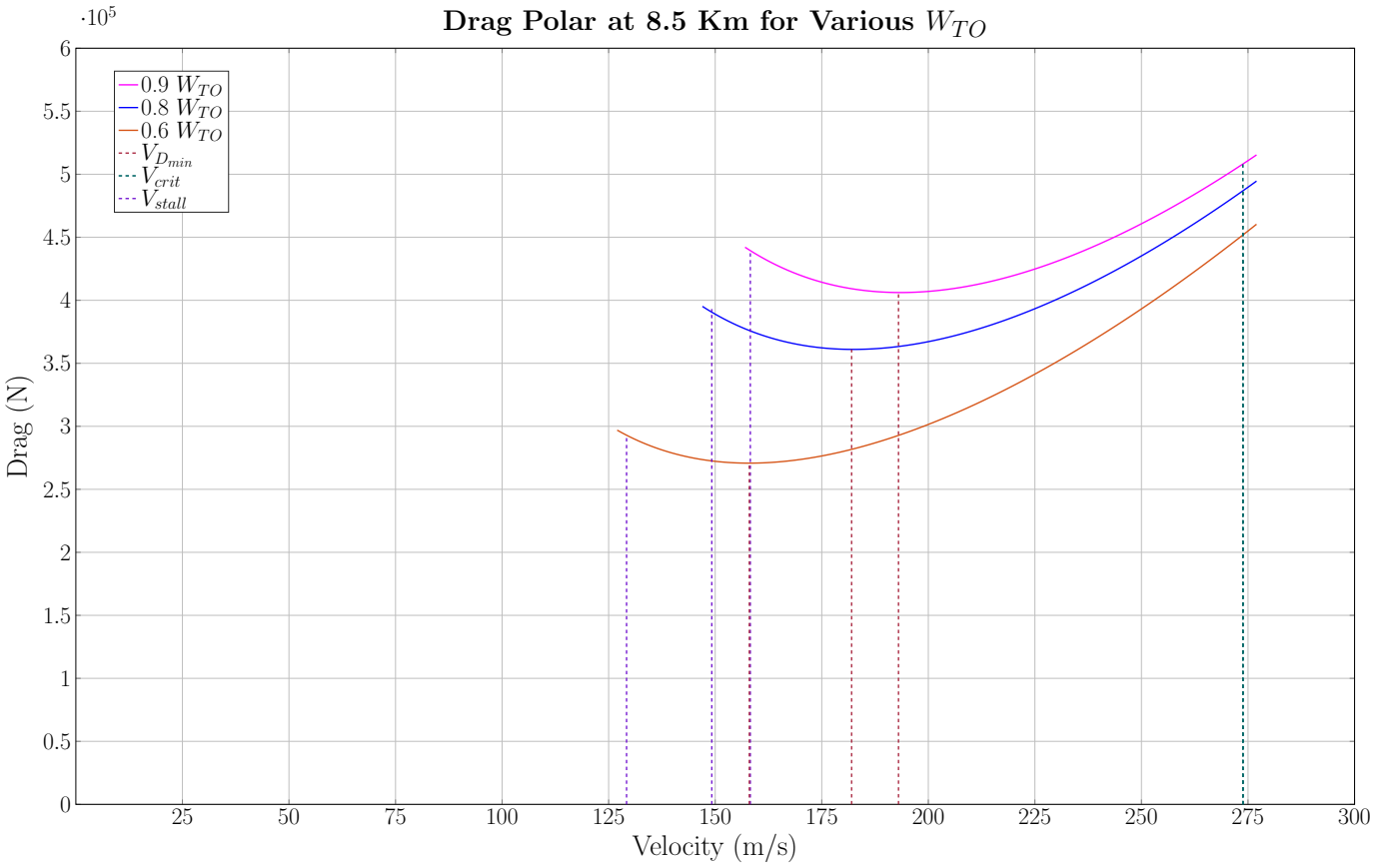

Parameter	Value
Altitude	0.5 km
V_{stall} at 0.9 W_{TO}	103.06 m/s
V_{stall} at 0.8 W_{TO}	97.17 m/s
V_{stall} at 0.6 W_{TO}	84.15 m/s
$V_{D_{min}}$ at 0.9 W_{TO}	156 m/s
$V_{D_{min}}$ at 0.8 W_{TO}	147 m/s
$V_{D_{min}}$ at 0.6 W_{TO}	127 m/s
V_{crit} at 0.9 W_{TO}	273.80 m/s
V_{crit} at 0.8 W_{TO}	273.80 m/s
V_{crit} at 0.6 W_{TO}	273.80 m/s

Table 8: Data for 8.5 km

2.9 Drag Polar for 10.5 km

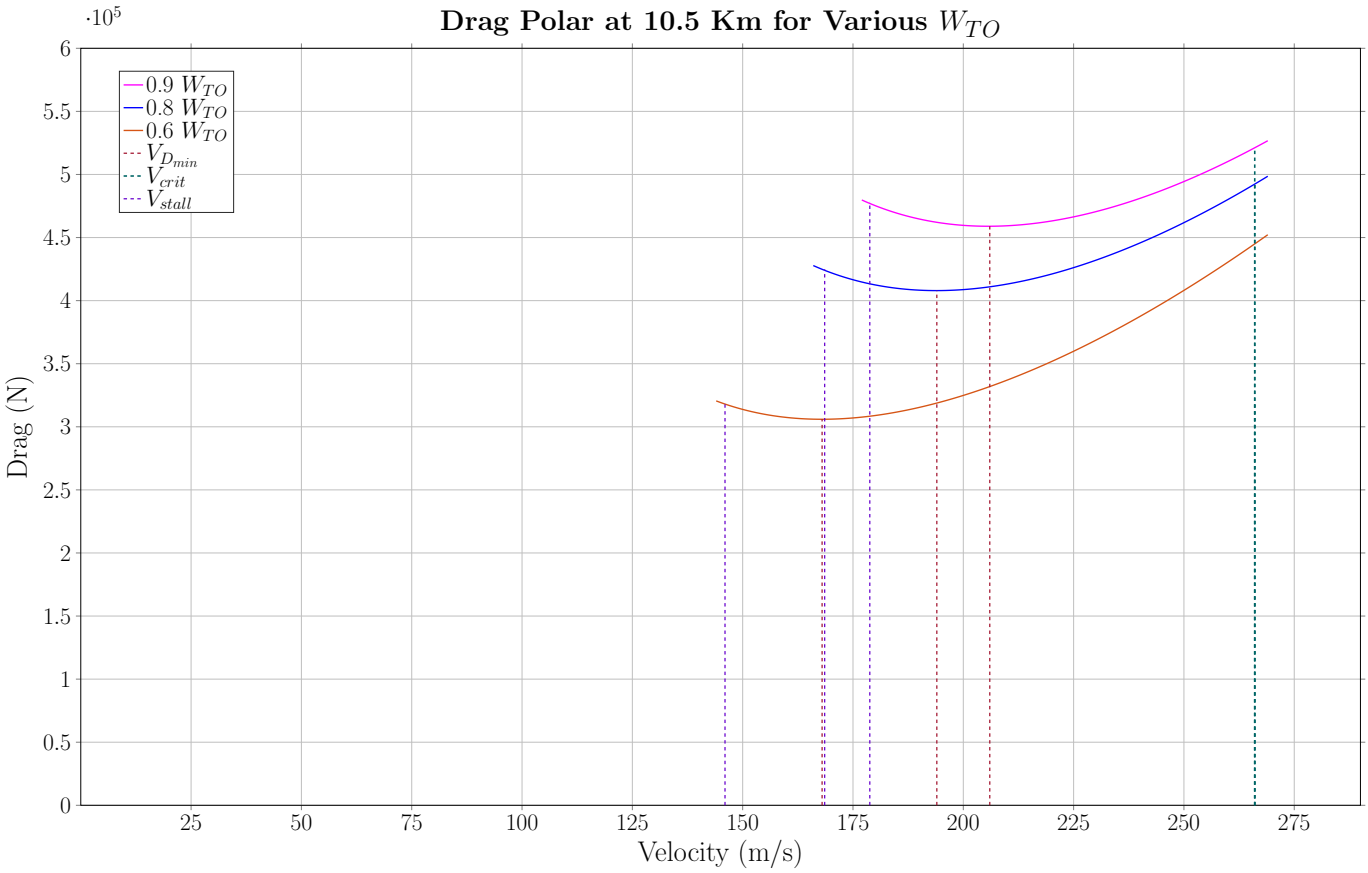

Parameter	Value
Altitude	0.5 km
V_{stall} at 0.9 W_{TO}	103.06 m/s
V_{stall} at 0.8 W_{TO}	97.17 m/s
V_{stall} at 0.6 W_{TO}	84.15 m/s
$V_{D_{min}}$ at 0.9 W_{TO}	156 m/s
$V_{D_{min}}$ at 0.8 W_{TO}	147 m/s
$V_{D_{min}}$ at 0.6 W_{TO}	127 m/s
V_{crit} at 0.9 W_{TO}	266.05 m/s
V_{crit} at 0.8 W_{TO}	266.05 m/s
V_{crit} at 0.6 W_{TO}	266.05 m/s

Table 9: Data for 10.5 km

2.10 Drag Polar for 11.5 km

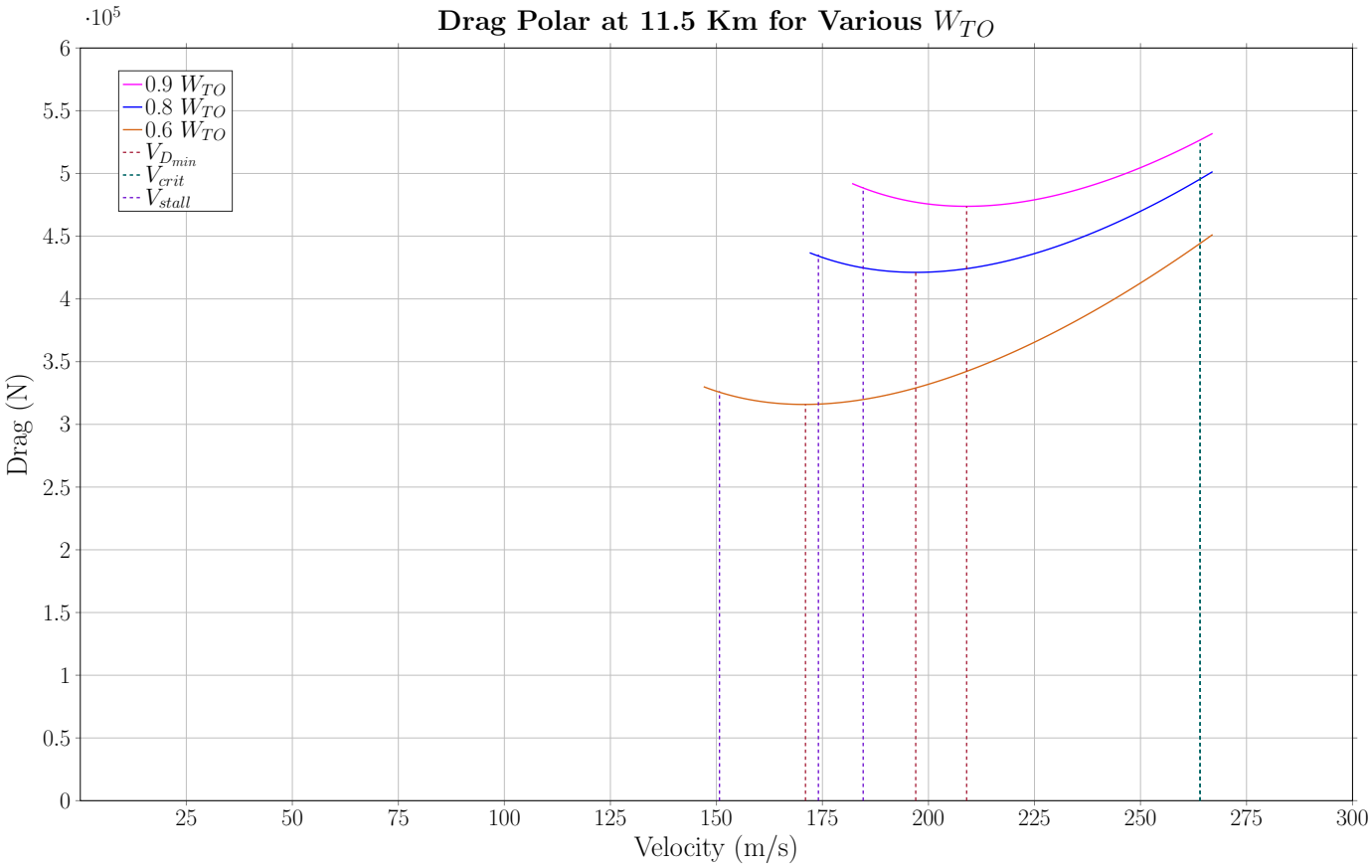

Parameter	Value
Altitude	0.5 km
V_{stall} at 0.9 W_{TO}	103.06 m/s
V_{stall} at 0.8 W_{TO}	97.17 m/s
V_{stall} at 0.6 W_{TO}	84.15 m/s
$V_{D_{min}}$ at 0.9 W_{TO}	156 m/s
$V_{D_{min}}$ at 0.8 W_{TO}	147 m/s
$V_{D_{min}}$ at 0.6 W_{TO}	127 m/s
V_{crit} at 0.9 W_{TO}	264.07 m/s
V_{crit} at 0.8 W_{TO}	264.07 m/s
V_{crit} at 0.6 W_{TO}	264.07 m/s

Table 10: Data for 11.5 km

2.11 Inferences

It is inferred that at constant take-off weight (W_{TO}), the minimum drag (D_{min}) is constant. Further, the critical velocity boundary (V_{crit}) is constant for a given altitude since it depends on the speed of sound at that respective altitude.

3 Flight Envelope (V-h Plot)

3.1 Preliminary Calculations

An aircraft's level flight envelope signifies the limits to which an aircraft must adhere at all times to maintain safe operational flight. It is a plot of the altitude (h) versus the velocity (V) and is used to determine the safe flight limits of an aircraft. The boundaries of this envelope are defined by the minimum and maximum velocities of the aircraft (V1 and V2, respectively).

The flight envelope and, in extension, the analysis of the aircraft at a given height and throttle setting was carried out for three take-off weights and six altitudes. The weights considered for the analysis were 0.9 W_{TO}, 0.8 W_{TO} and 0.6 W_{TO}.

The altitudes at which the drag was estimated were 0.5 km, 3 km, 5.5 km, 8.5 km, 10.5 km and 11.5 km. On each polar, the V_{stall},q_{max} and the V_{crit} boundaries were marked to signify the flight envelope limits.

The equation for level, steady flight,

$$D = AV^2 + {}^{B}\!/_{V^2} = T_{ASL}\sigma^m \tag{8}$$

where A = ${}^{C_{D_0}\rho S}\!/_{2}$ and B = ${}^{2kW^2}\!/_{\rho S}$. T_{ASL} is the thrust at sea level, σ is the density ratio and m ≤ 1. A quadratic equation in V^2 is obtained,

$$AV^4 - \left(T_{ASL}\sigma^m\right)V^2 + B = 0 \tag{9}$$

Solving this, two values of V are obtained,

$$V^2 = \frac{\left(T_{ASL}\sigma^m\right) \pm \sqrt{\left(\left(T_{ASL}\sigma^m\right) - 4AB\right.}}{2A} \tag{10}$$

At the absolute ceiling, we get one velocity value if,

$$\left(T_{ASL}\sigma_{abs}^m\right)^2 = 4AB = 4kC_{D_0}W^2 \tag{11}$$

From equation 11 we get σ_{abs} as,

$$\sigma_{abs} = \frac{2\sqrt{kC_{D_0}}}{\left({}^{T_{ASL}}\!/_{W}\right)^m} \tag{12}$$

From the above equation, the density of that particular altitude can be obtained by,

$$\sigma = \frac{\rho_h}{\rho_{SL}} \tag{13}$$

Hence, the absolute altitude can be calculated from the density at the altitude using ISA.
The dynamic head (q) is given by,

$$q = \frac{1}{2}\rho V^2 \tag{14}$$

To plot the aeroelastic or the q_{max} boundary, the density is varied based on altitude, and the velocity can be obtained since $q = q_{max}$ is constant.

The stall velocity V_{stall} was calculated using the relation,

$$V_{stall} = \sqrt{\frac{2W_{TO}}{\rho S C_{L_{max}}}} \tag{15}$$

The critical velocity (V_{crit}) was calculated from the initial value at sea level by varying the speed of sound according to the altitude.

3.2 V-h Plot for 0.9 W_{TO} and 100% Throttle

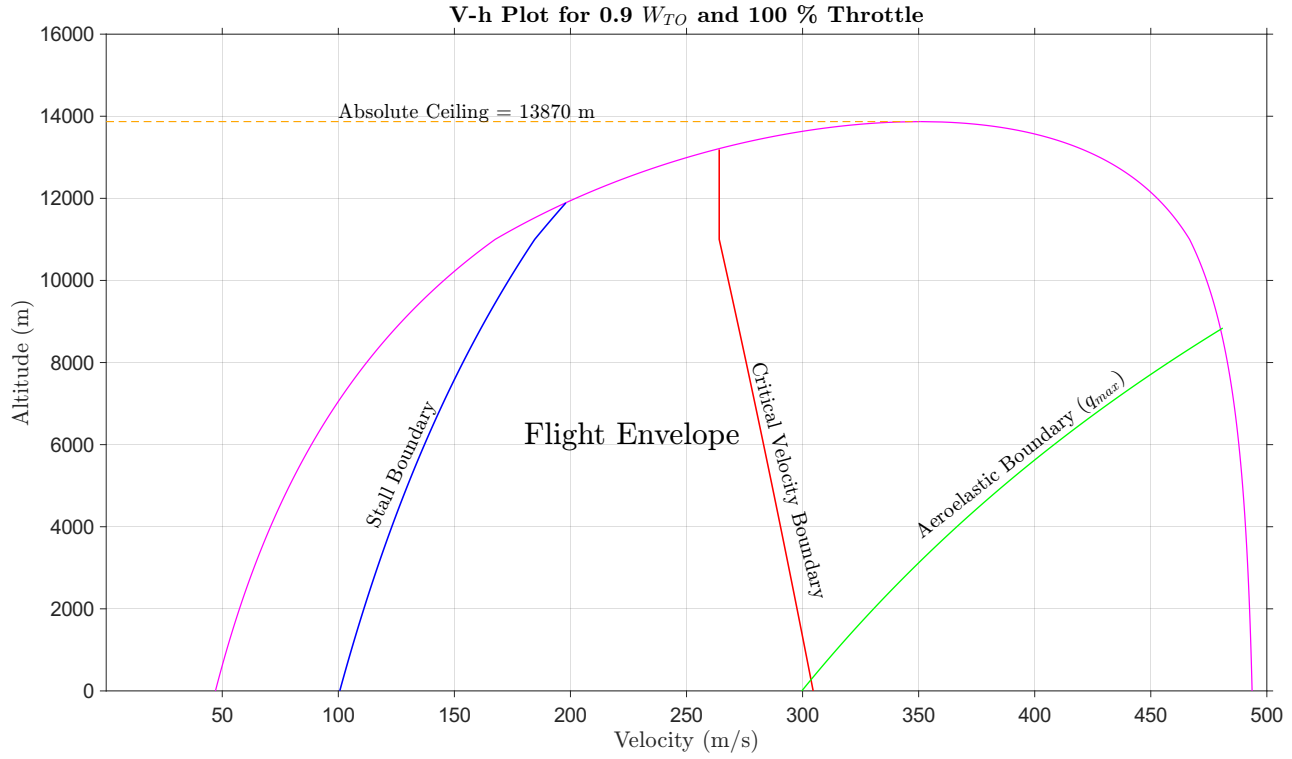

3.3 V-h Plot for 0.8 W_{TO} and 100% Throttle

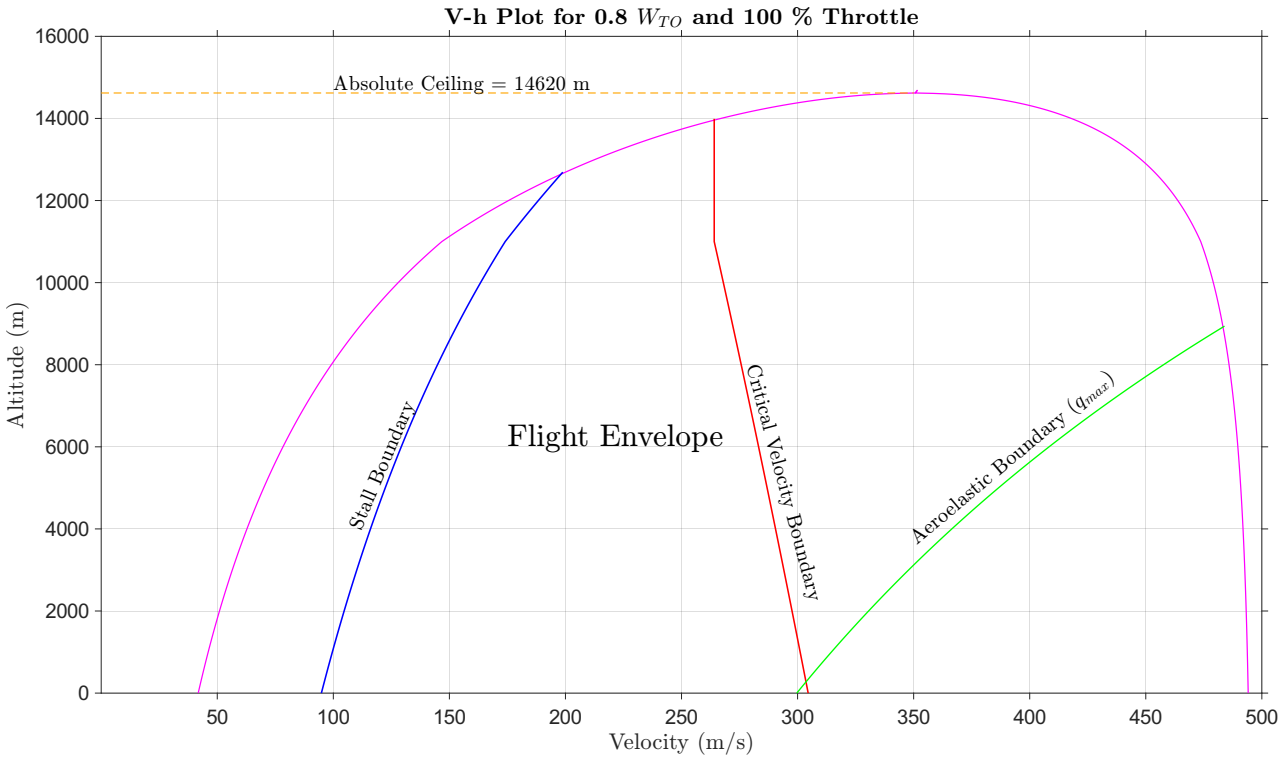

3.4 V-h Plot for 0.6 W_{TO} and 100% Throttle

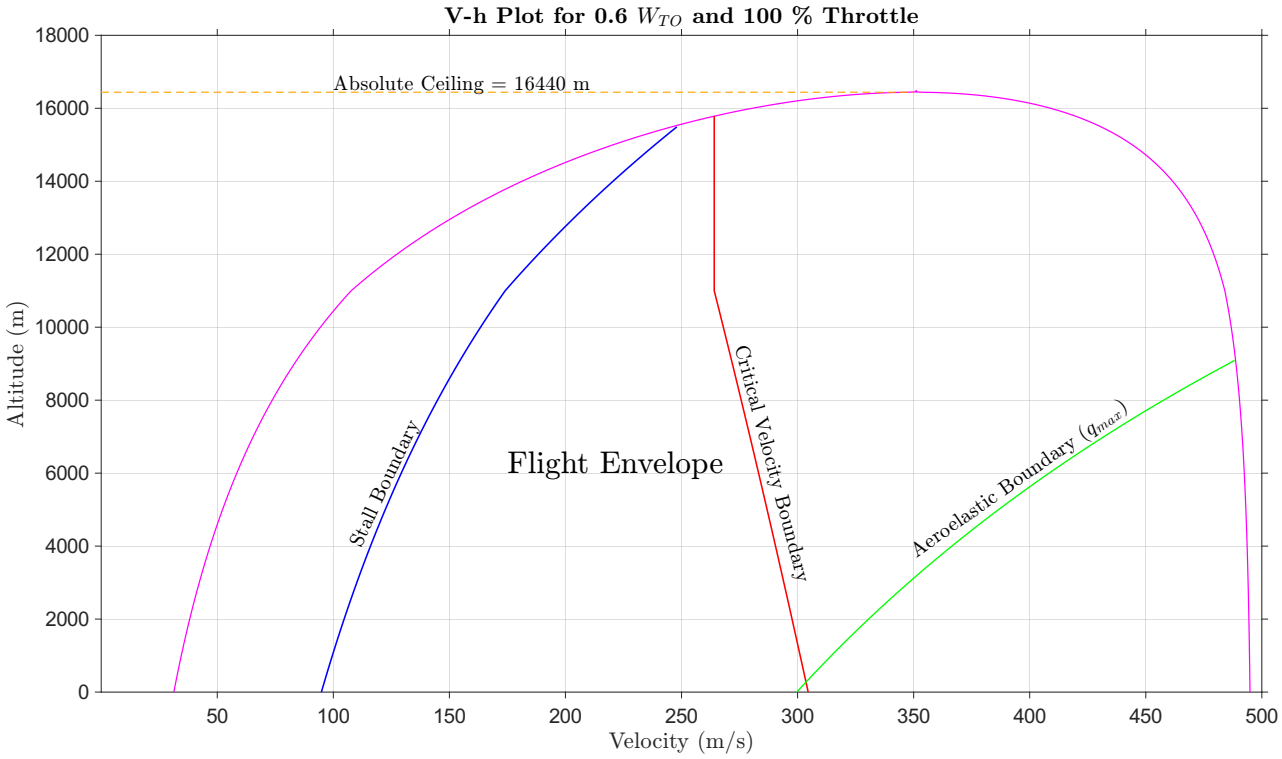

3.5 V-h Plot for 0.9 W_{TO} and 95% Throttle

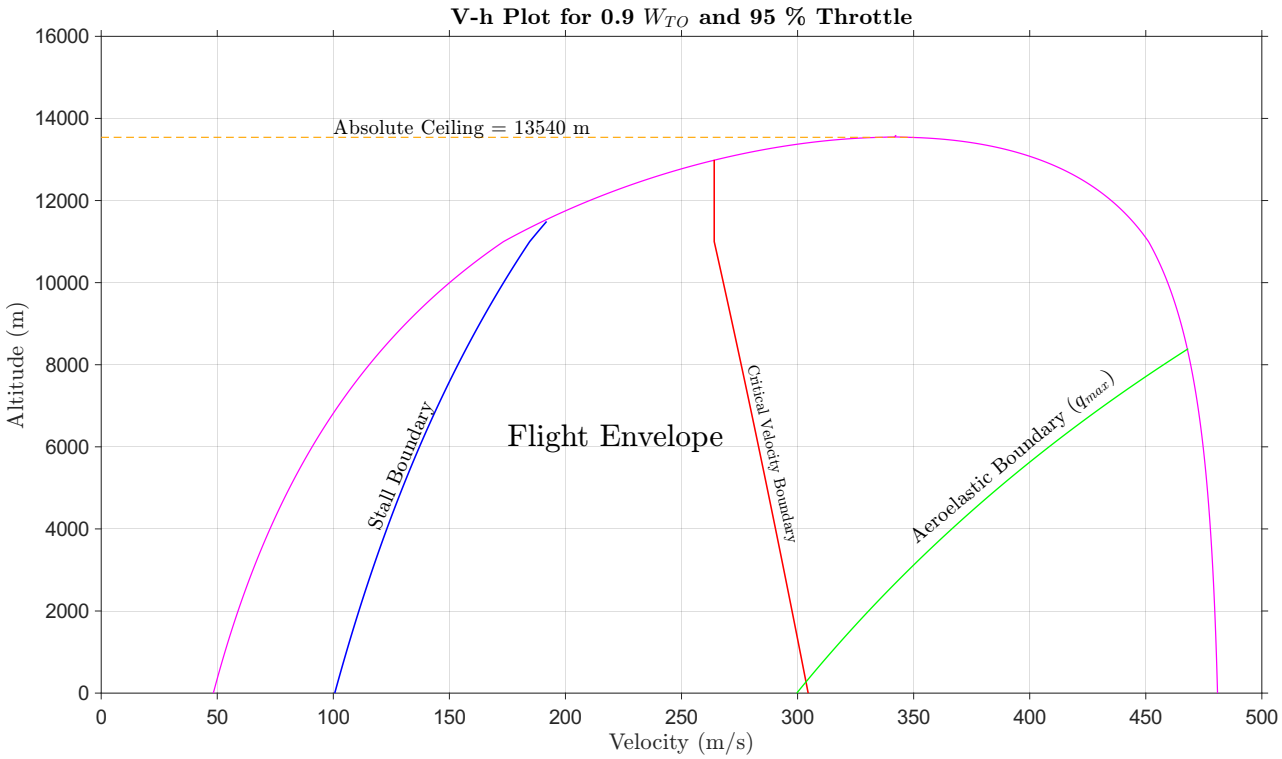

3.6 V-h Plot for 0.9 W_{TO} and 82.5% Throttle

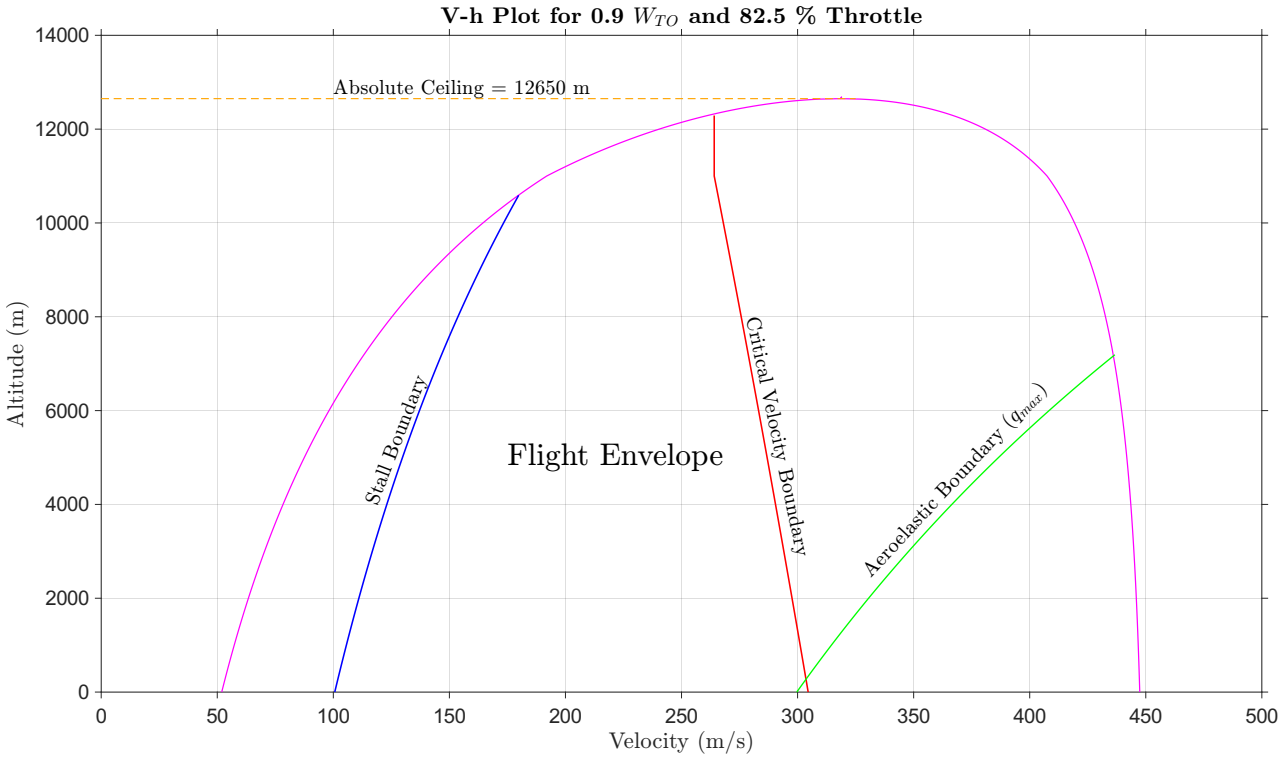

3.7 V-h Plot for 0.9 W_{TO} and 70% Throttle

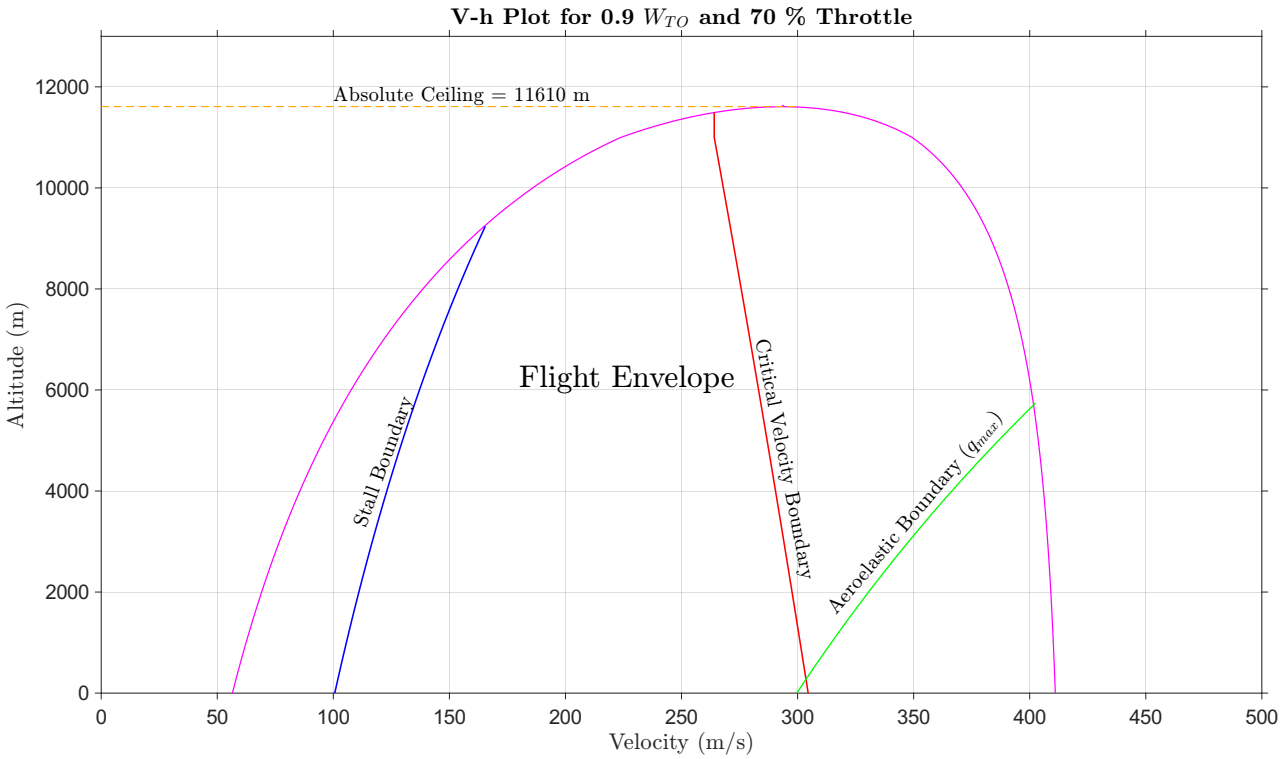

3.8 Combined V-h Plot for 0.9 W_{TO}

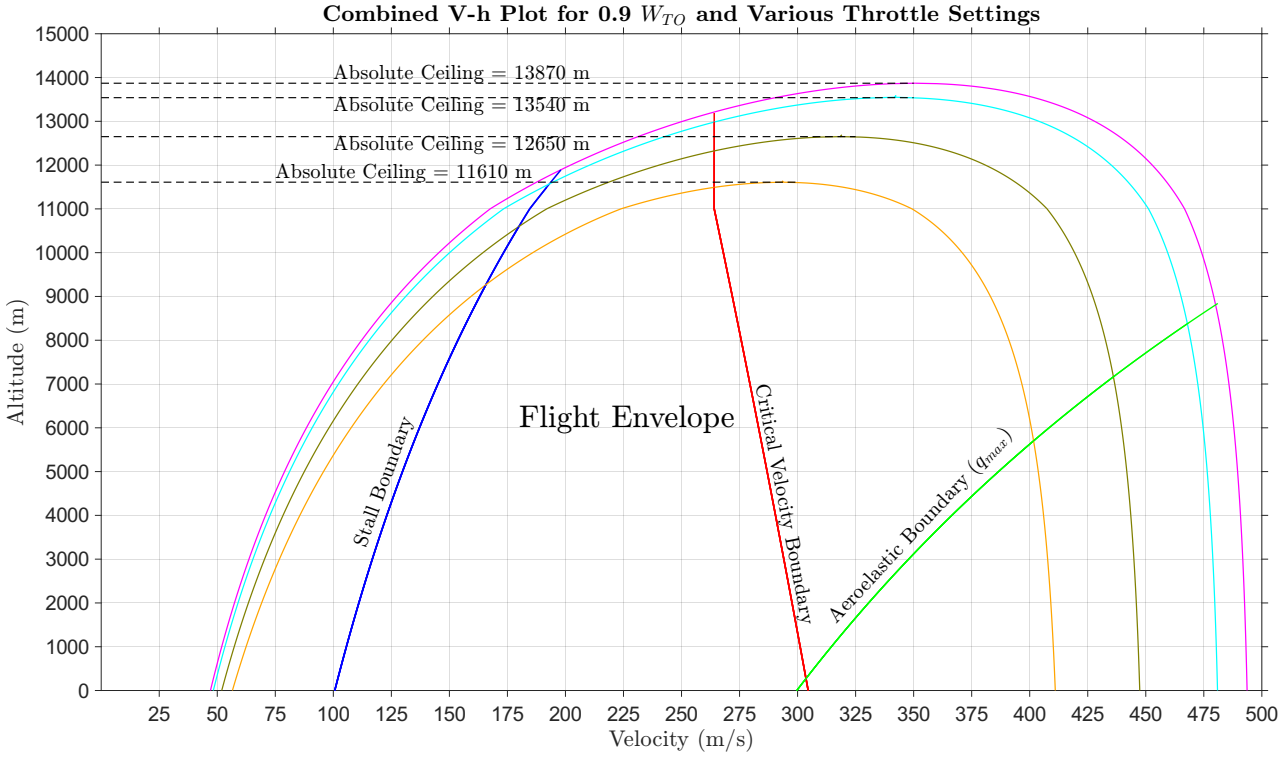

3.9 Inferences

It is inferred that the absolute ceiling (h_{abs}) varies with a change in take-off weight W_{TO} and the throttle percentage. The absolute ceiling (h_{abs}) is inversely proportional to take-off weight W_{TO} and directly proportional to the throttle percentage.

4 Rate Of Climb (R/C)

4.1 Preliminary Calculations

The rate of climb and, by extension, the analysis of the aircraft at a given height was carried out for three take-off weights and six altitudes. The weights considered for the analysis were 0.9 W_{TO}, 0.8 W_{TO} and 0.6 W_{TO}.

The altitudes at which the drag was estimated were 0.5 km, 3 km, 5.5 km, 8.5 km, 10.5 km and 11.5 km. The V_{stall} and the V_{crit} boundaries were marked to signify the flight envelope limits on each polar. The throttle setting for the plots in this section was considered to be 100%

The power available for flight (P_{avb}) is given by,

$$P_{avb} = Thrust \times V \tag{16}$$

The power required for flight (P_{reqd}) is given by,

$$P_{reqd} = Drag \times V \tag{17}$$

The power difference for flight (ΔP) is given by,

$$\Delta P = P_{avb} - P_{reqd} \tag{18}$$

Hence the Rate of Climb (R/C) can be obtained as,

$$R/C = \frac{\Delta P}{W} \tag{19}$$

The Best Rate of Climb at a given altitude is the maximum rate of climb corresponding to that altitude. The Best Rate of Climb from sea level (SL) to an altitude, say h, is given by,

$$(R/C)_{SL \to h} = \frac{(R/C)_{SL} + (R/C)_h}{2} \tag{20}$$

The density ratio at the absolute altitude σ_{abs} can be written as,

$$\sigma_{abs} = \frac{2\sqrt{kC_{D_0}}}{\left(T_{ASL}/W\right)^m} \tag{21}$$

From the above equation, the density of that particular altitude can be obtained by,

$$\sigma = \frac{\rho_h}{\rho_h} \tag{22}$$

Hence, the absolute altitude can be calculated from the density at the altitude using ISA. The stall velocity V_{stall} was calculated using the relation,

$$V_{stall} = \sqrt{\frac{2W_{TO}}{\rho S C_{L_{max}}}} \tag{23}$$

The critical velocity (V_{crit}) was calculated from the initial value at sea level by varying the speed of sound according to the altitude.

The time to climb can be calculated from the relation,

$$t = \int_a^b \frac{1}{(R/C)_{max}} \tag{24}$$

where a is the current altitude and b is the final altitude.

4.2 Rate Of Climb Plot for 0.9 W_{TO}

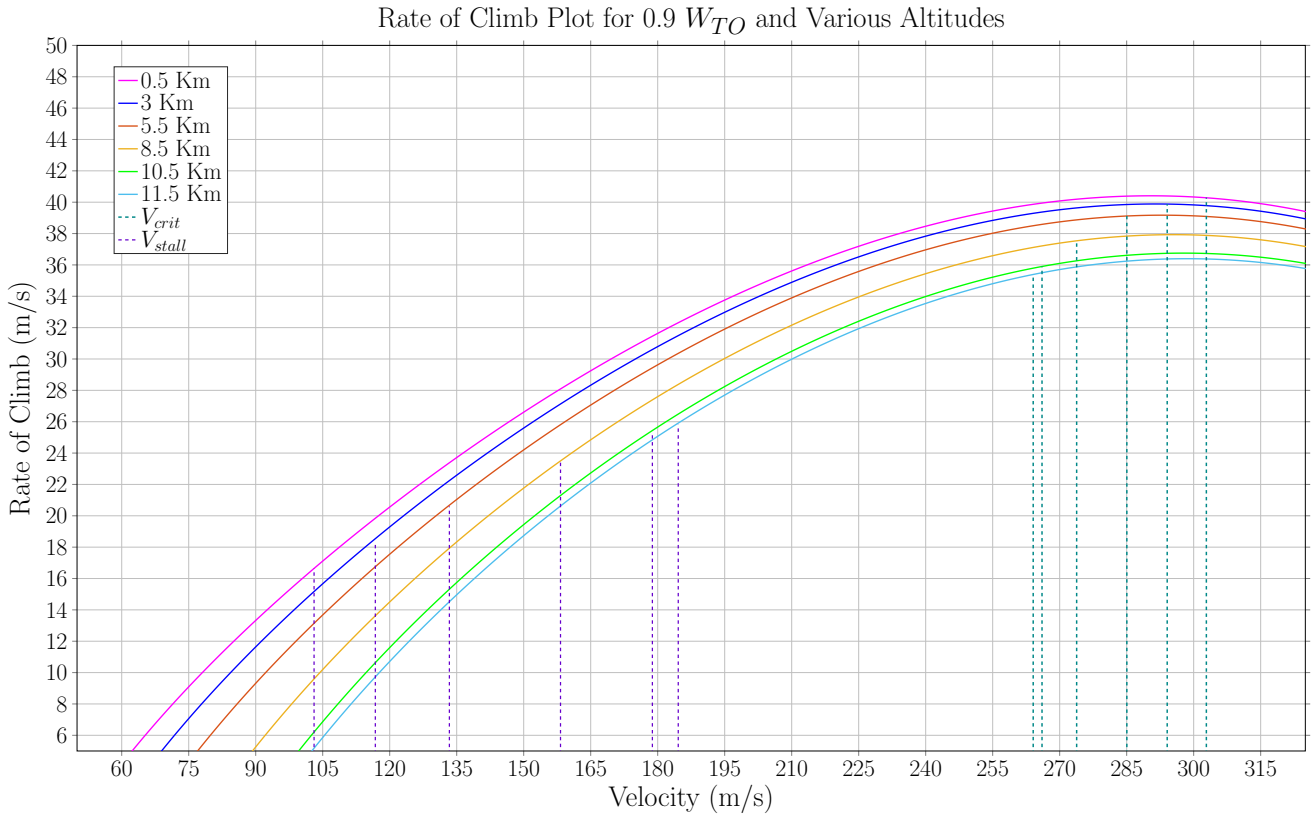

Parameter	Value
Take-off Weight (W_{TO})	6025.5 kN
V_{stall} at 0.5 km	103.06 m/s
V_{stall} at 3 km	116.78 m/s
V_{stall} at 5.5 km	133.36 m/s
V_{stall} at 8.5 km	158.24 m/s
V_{stall} at 10.5 km	178.81 m/s
V_{stall} at 11.5 km	184.60 m/s

Parameter	Value
Take-off Weight (W_{TO})	6025.5 kN
V_{crit} at 0.5 km	302.84 m/s
V_{crit} at 3 km	294.07 m/s
V_{crit} at 5.5 km	285.04 m/s
V_{crit} at 8.5 km	273.80 m/s
V_{crit} at 10.5 km	266.05 m/s
V_{crit} at 11.5 km	264.07 m/s

Table 11: Data for 0.9 W_{TO}

4.3 Rate Of Climb Plot for 0.8 W_{TO}

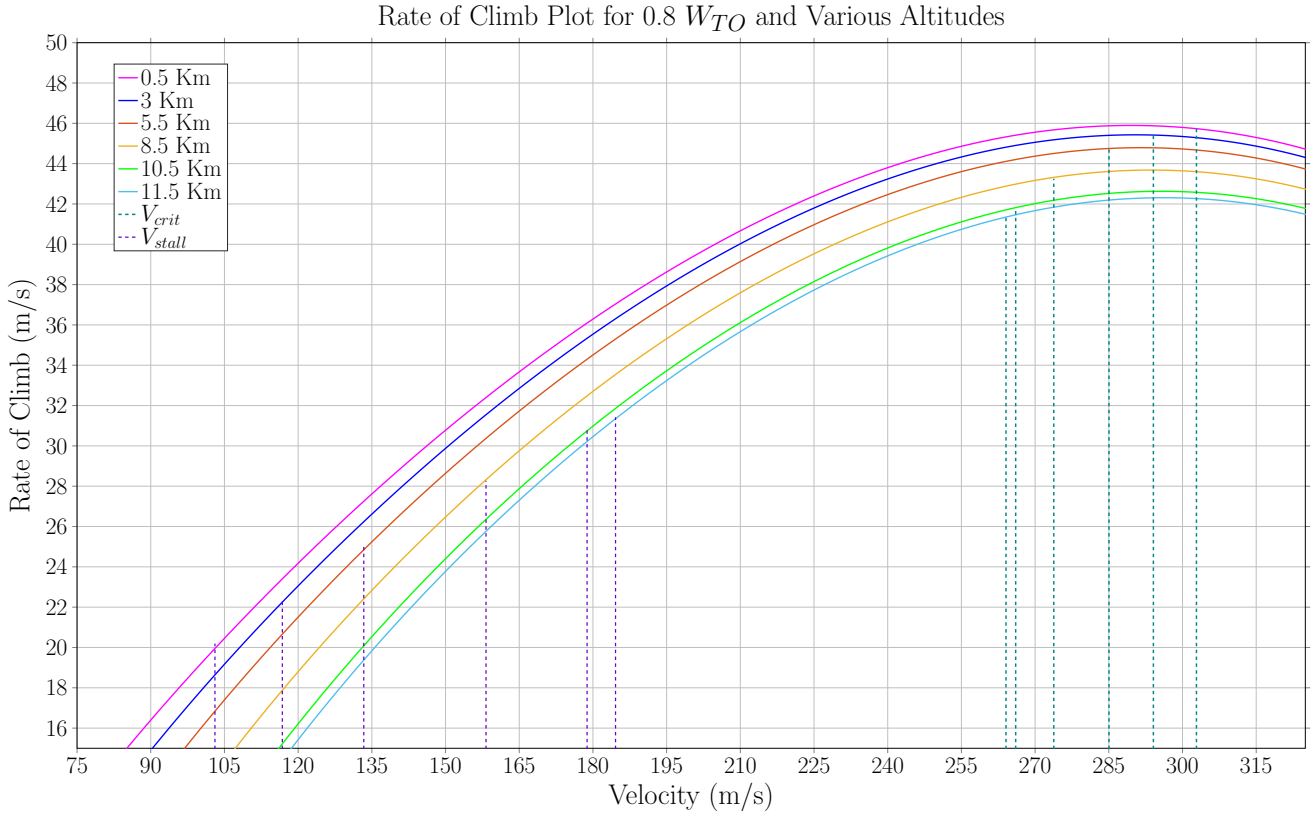

Parameter	Value
Take-off Weight (W_{TO})	5356 kN
V_{stall} at 0.5 km	97.17 m/s
V_{stall} at 3 km	110.10 m/s
V_{stall} at 5.5 km	125.73 m/s
V_{stall} at 8.5 km	149.19 m/s
V_{stall} at 10.5 km	168.58 m/s
V_{stall} at 11.5 km	174.04 m/s

Parameter	Value
Take-off Weight (W_{TO})	5356 kN
V_{crit} at 0.5 km	302.84 m/s
V_{crit} at 3 km	294.07 m/s
V_{crit} at 5.5 km	285.04 m/s
V_{crit} at 8.5 km	273.80 m/s
V_{crit} at 10.5 km	266.05 m/s
V_{crit} at 11.5 km	264.07 m/s

Table 12: Data for 0.8 W_{TO}

4.4 $(R/C)_{max}$ for 0.9 W_{TO}

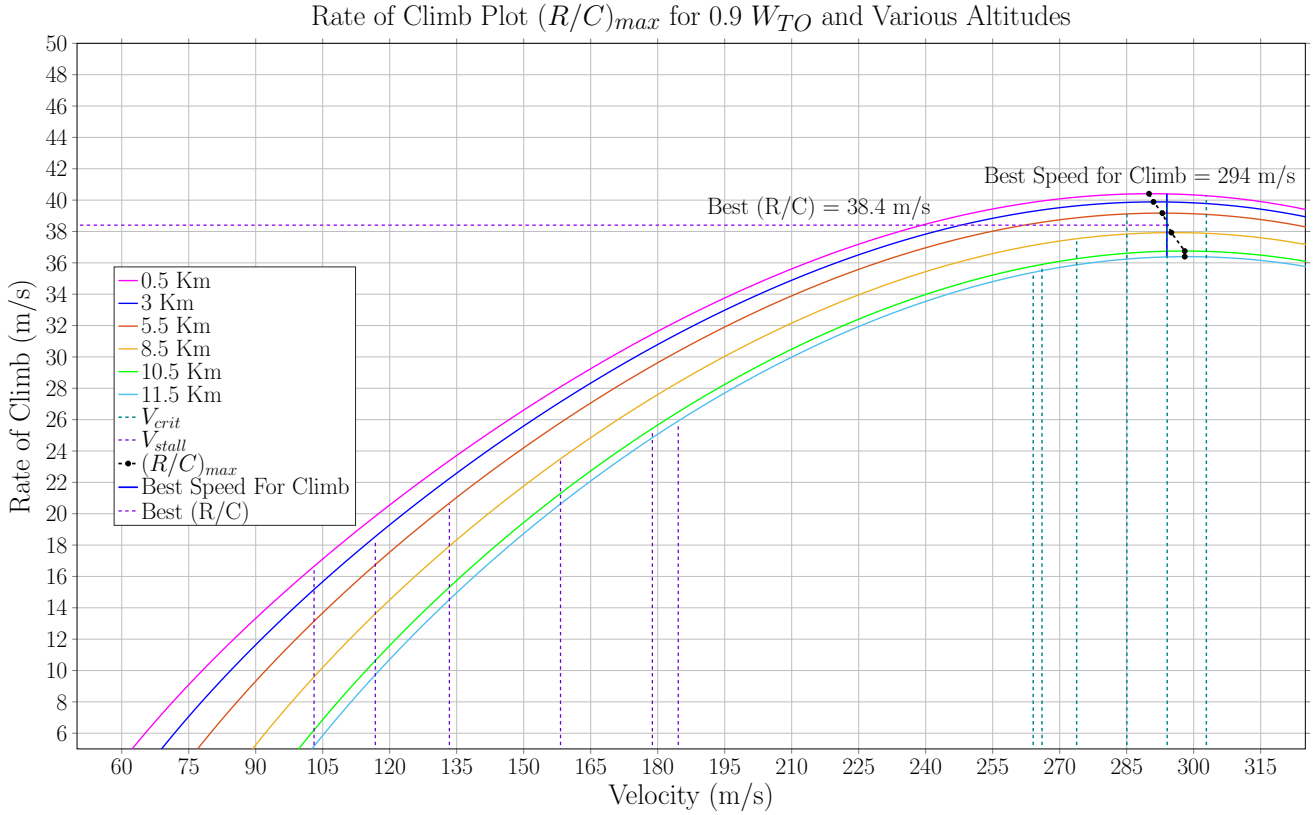

Parameter	Value
Take-off Weight (W_{TO})	6025.5 kN
V_{stall} at 0.5 km	103.06 m/s
V_{stall} at 3 km	116.78 m/s
V_{stall} at 5.5 km	133.36 m/s
V_{stall} at 8.5 km	158.24 m/s
V_{stall} at 10.5 km	178.81 m/s
V_{stall} at 11.5 km	184.60 m/s
$(R/C)_{max}$ at 0.5 km	40.41 m/s
$(R/C)_{max}$ at 3 km	39.88 m/s
$(R/C)_{max}$ at 5.5 km	39.17 m/s

Parameter	Value
Take-off Weight (W_{TO})	6025.5 kN
$(R/C)_{max}$ at 8.5 km	37.92 m/s
$(R/C)_{max}$ at 10.5 km	36.75 m/s
$(R/C)_{max}$ at 11.5 km	36.39 m/s
V_{crit} at 0.5 km	302.84 m/s
V_{crit} at 3 km	294.07 m/s
V_{crit} at 5.5 km	285.04 m/s
V_{crit} at 8.5 km	273.80 m/s
V_{crit} at 10.5 km	266.05 m/s
V_{crit} at 11.5 km	264.07 m/s

Table 13: Data for 0.9 W_{TO}

4.5 $(R/C)_{max}$ for 0.8 W_{TO}

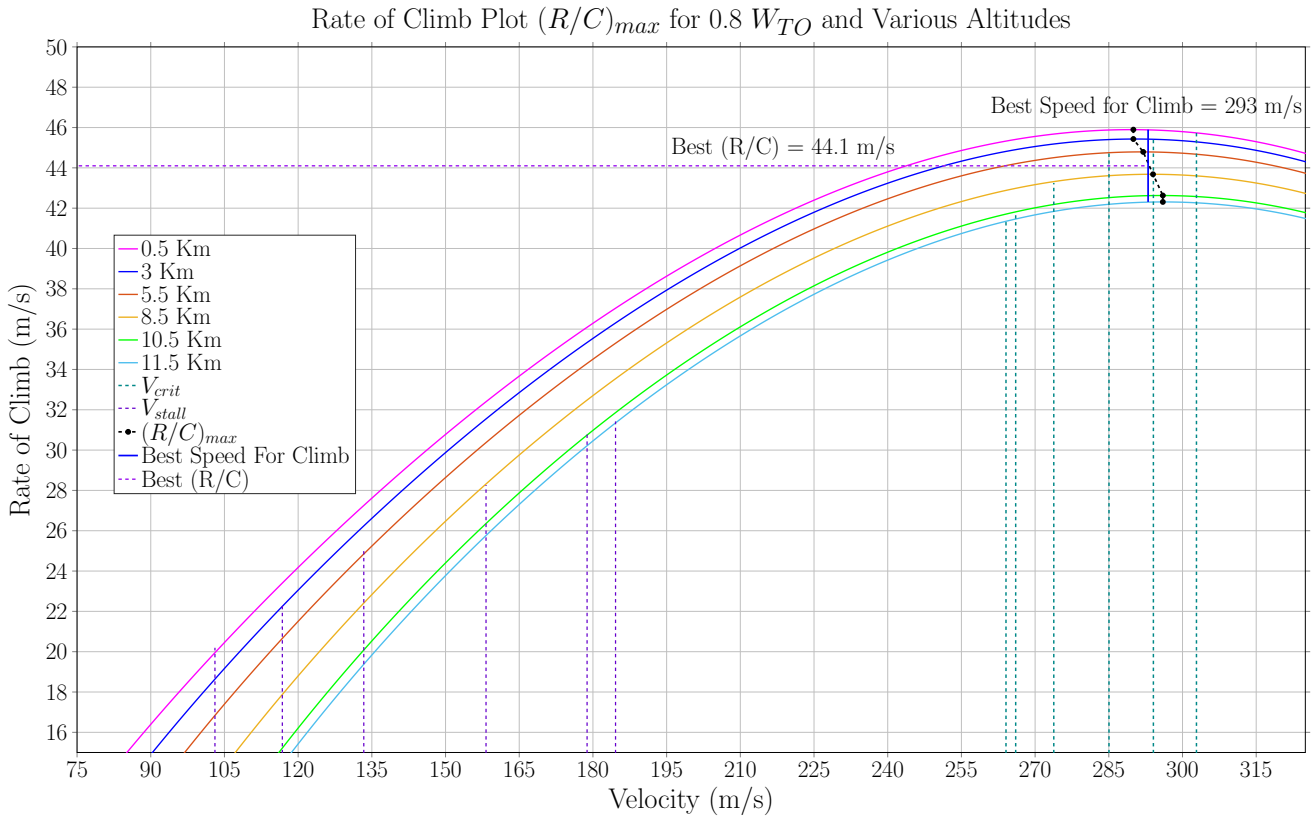

Parameter	Value
Take-off Weight (W_{TO})	5356 kN
V_{stall} at 0.5 km	97.17 m/s
V_{stall} at 3 km	110.10 m/s
V_{stall} at 5.5 km	125.73 m/s
V_{stall} at 8.5 km	149.19 m/s
V_{stall} at 10.5 km	168.58 m/s
V_{stall} at 11.5 km	174.04 m/s
$(R/C)_{max}$ at 0.5 km	45.89 m/s
$(R/C)_{max}$ at 3 km	45.43 m/s
$(R/C)_{max}$ at 5.5 km	44.79 m/s

Parameter	Value
Take-off Weight (W_{TO})	5356 kN
$(R/C)_{max}$ at 8.5 km	43.68 m/s
$(R/C)_{max}$ at 10.5 km	42.63 m/s
$(R/C)_{max}$ at 11.5 km	42.31 m/s
V_{crit} at 0.5 km	302.84 m/s
V_{crit} at 3 km	294.07 m/s
V_{crit} at 5.5 km	285.04 m/s
V_{crit} at 8.5 km	273.80 m/s
V_{crit} at 10.5 km	266.05 m/s
V_{crit} at 11.5 km	264.07 m/s

Table 14: Data for 0.8 W_{TO}

4.6 h v/s $(R/C)_{max}$ for 0.9 W_{TO}

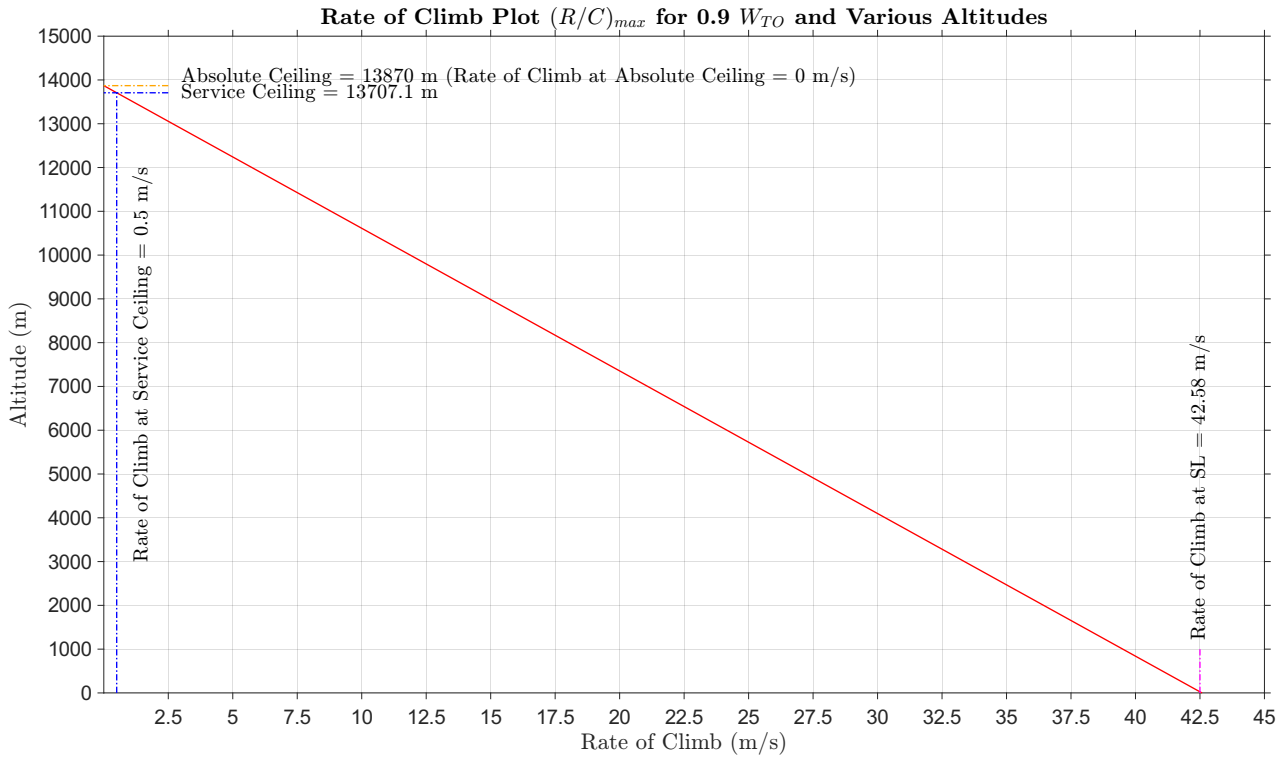

4.7 h v/s $(R/C)_{max}$ for 0.8 W_{TO}

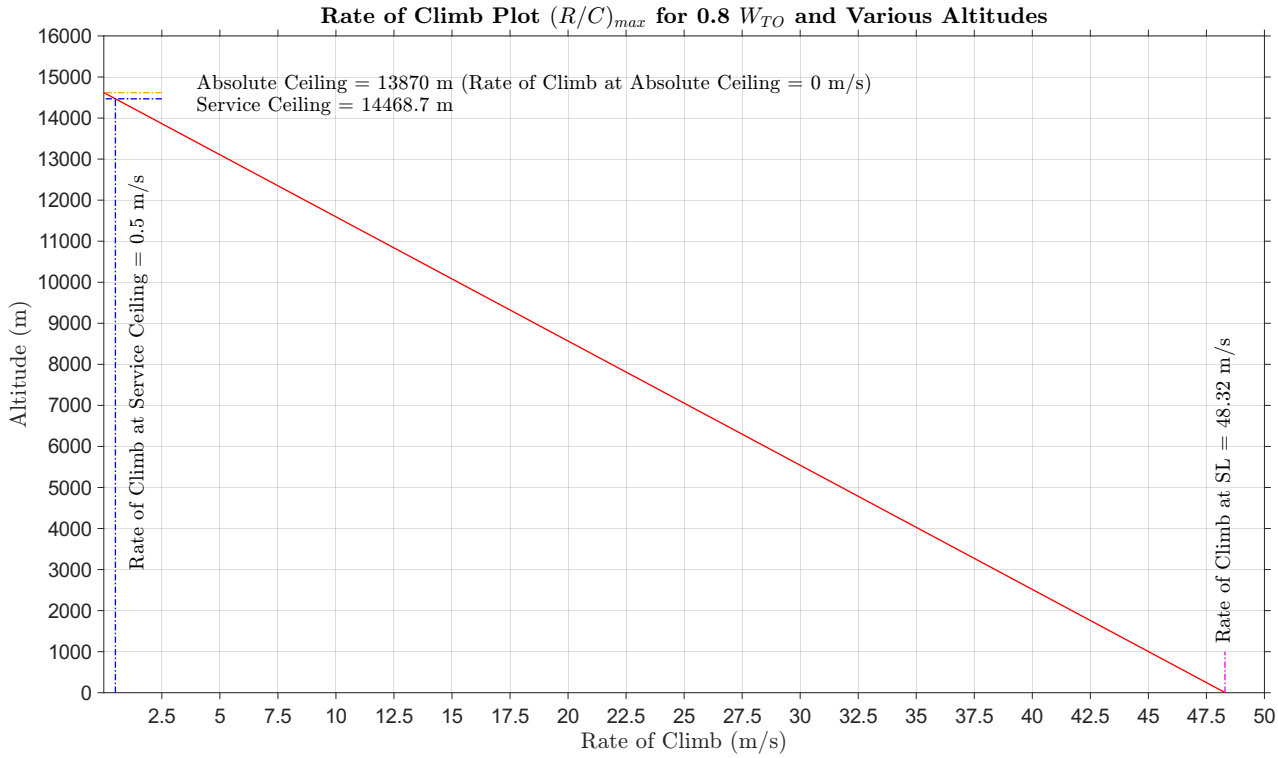

4.8 Thrust v/s Altitude for 0.9 W_{TO}

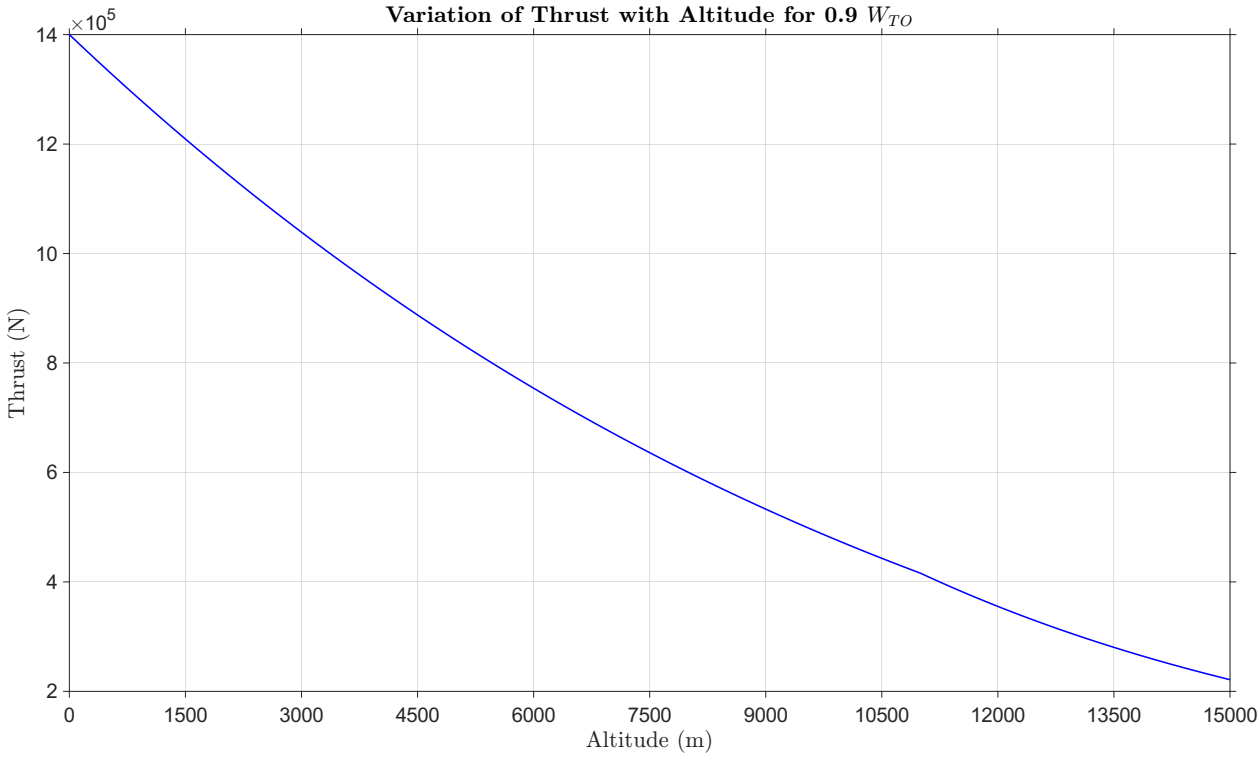

4.9 TSFC v/s Altitude for 0.9 W_{TO}

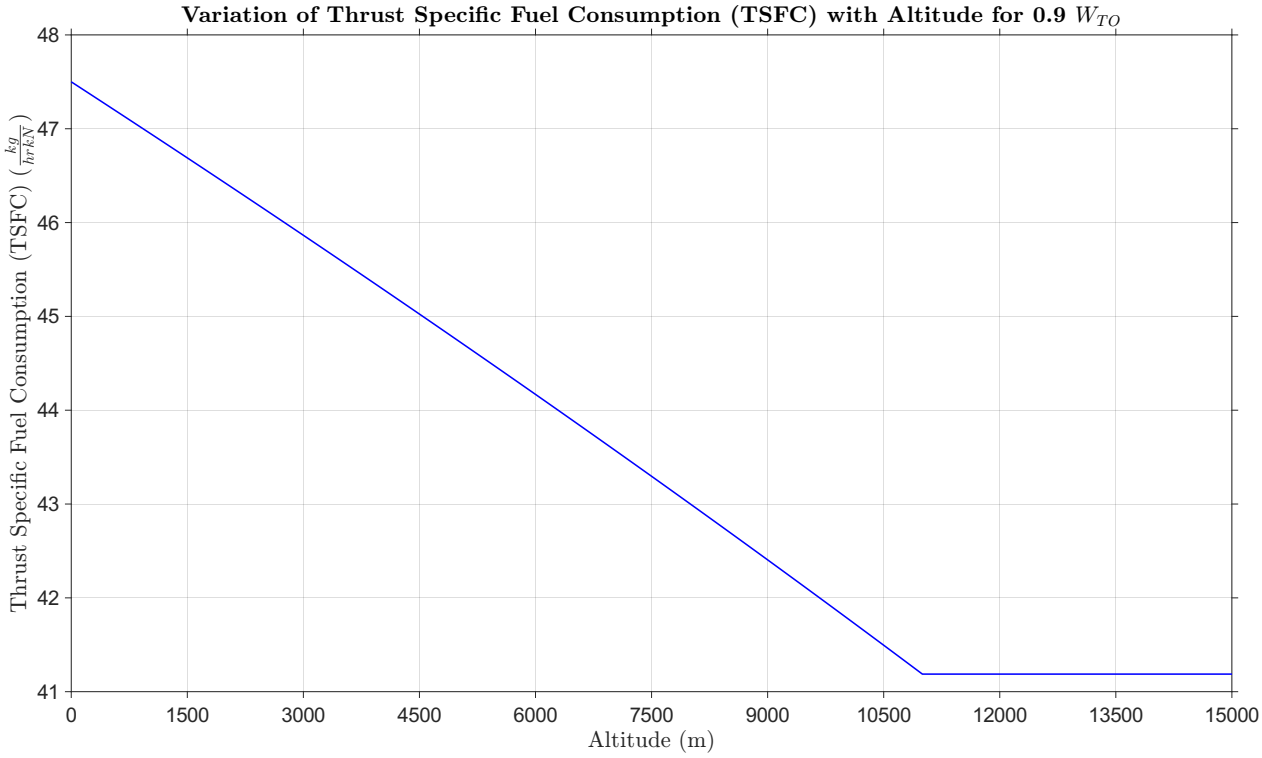

4.10 Variation of Altitude with Time ($\Sigma\Delta t_i$) for 0.9 W_{TO}

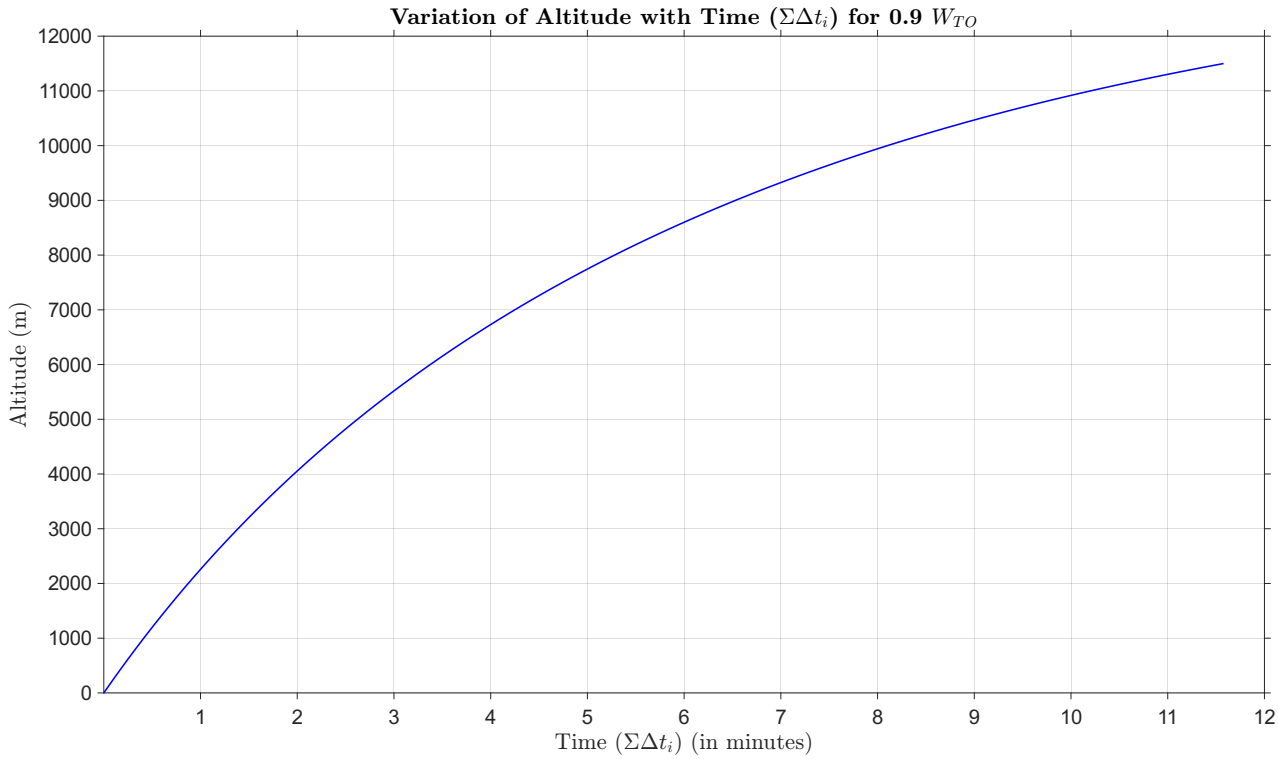

4.11 Variation of Weight (W_i) with Altitude for 0.9 W_{TO}

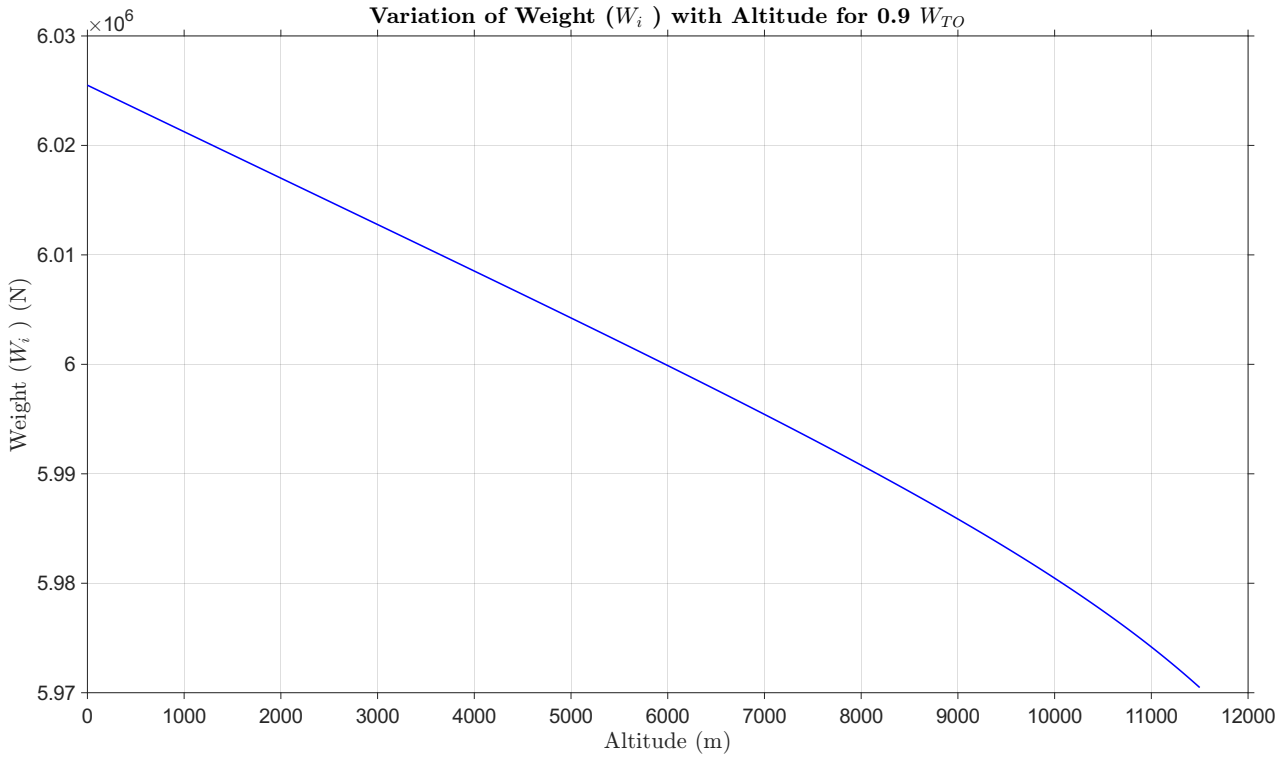

4.12 Variation of Change in Weight ($\Sigma\Delta W_{fi}$) with Altitude for 0.9 W_{TO}

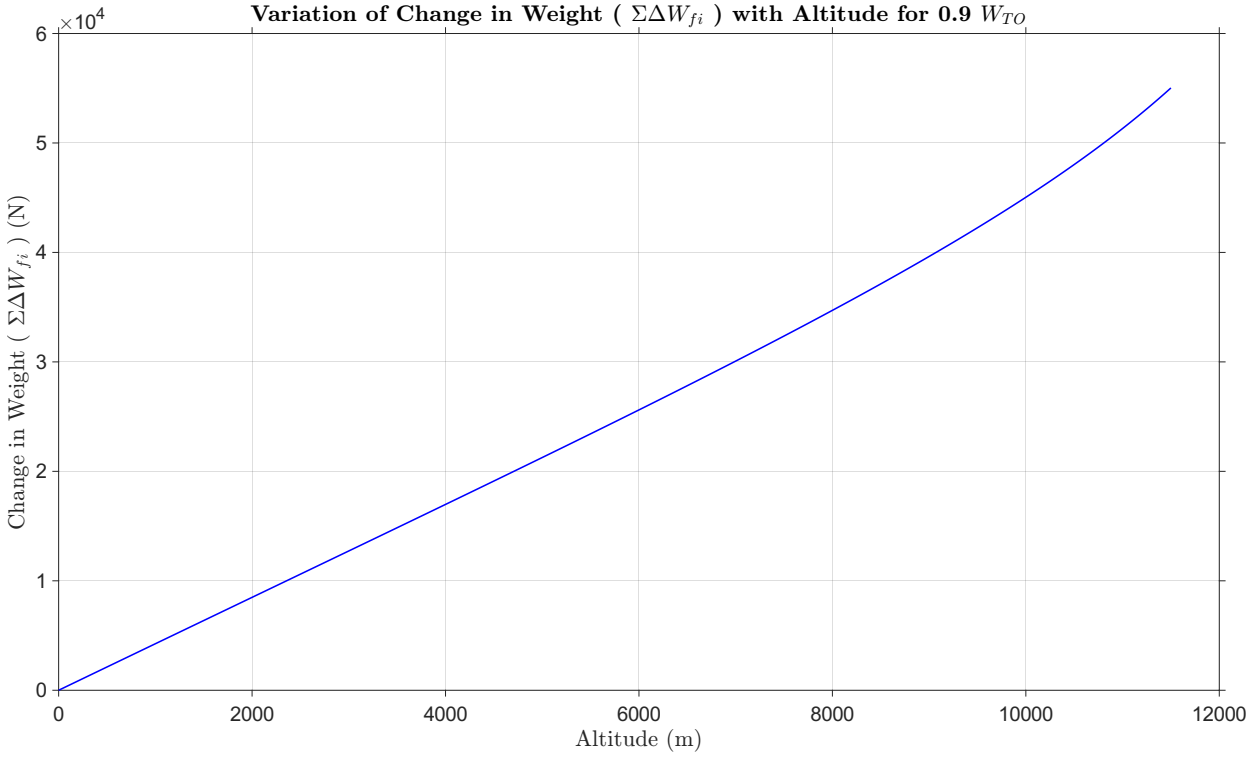

4.13 Variation of sin γ_i with Altitude for 0.9 W_{TO}

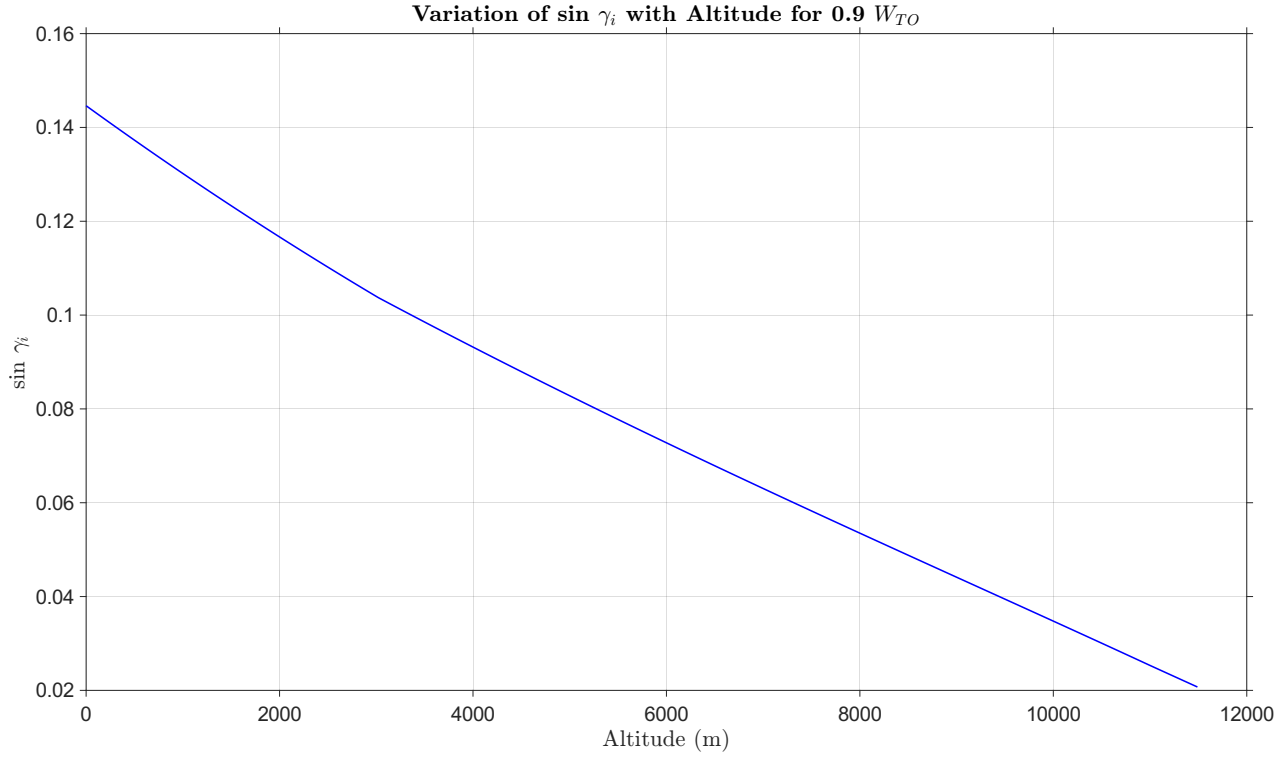

4.14 Variation of R/C with Altitude for 0.9 W_{TO}

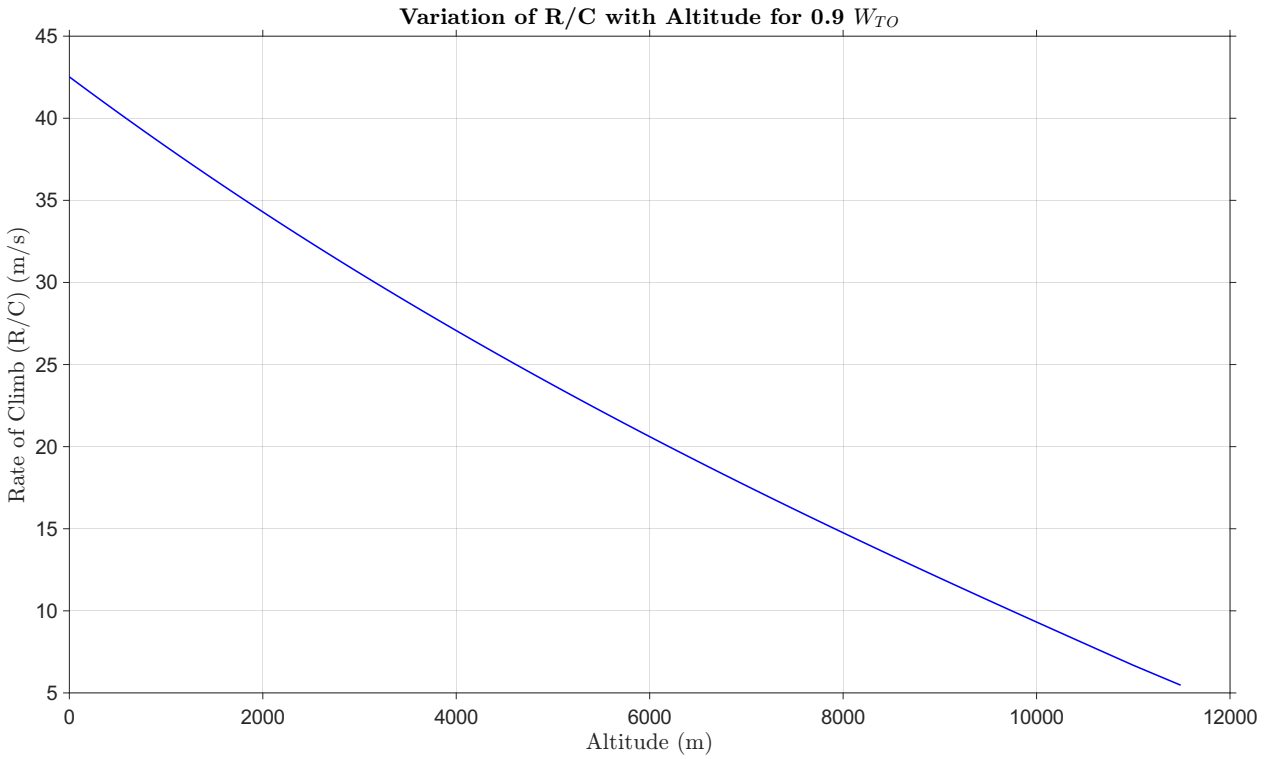

4.15 Time to Climb and Fuel to Climb

The estimation of the fuel to climb and the time to climb was done using the iterative method described in reference 4 (see the reference section). The formulae used in this approach are (for climb segments i = 1 to N),

$$\Delta h = h/N \tag{25}$$

From ISA,

$$h_i = 44300(1 - \sigma_i^{0.235}) \tag{26}$$

Hence,

$$\sigma_i = [1 - (h_i/44300)]^{\frac{1}{0.235}} \tag{27}$$

Hence the dynamic pressure (q) can be quantified as,

$$q_i = \sigma_i q_{SL} \tag{28}$$

From ISA,

$$\theta_i = \frac{(288.16 - 0.0065h_i)}{288.16} \tag{29}$$

The thrust-specific fuel consumption for a turbofan aircraft (c_T) can be calculated using,

$$(c_T)_i = (c_T)_{SL}\sqrt{\theta} \tag{30}$$

The weights for i = 1 to i = n-1 are given by,

$$W_1 = W_0 \tag{31}$$

and,

$$W_{i+1} = W_i - (\Delta W_f)_i \tag{32}$$

Thus C_L can be calculated,

$$(C_L)_i = \frac{W_i}{q_i S} \tag{33}$$

Further, C_D can be calculated,

$$(C_D)_i = C_{D_0} + k(C_{L_i})^2 \tag{34}$$

From C_D, the drag can be calculated as,

$$D_i = C_{D_i} q_i S \tag{35}$$

To calculate the rate of climb,

$$sin(\gamma_i) = \frac{[T_{SL}\sigma_i - D_i]}{W_i} \tag{36}$$

Hence,

$$(R/C)_i = V sin(\gamma_i) \tag{37}$$

The incremental time is given by,

$$\Delta t_i = \frac{\Delta h}{(R/C)_i} \tag{38}$$

The incremental fuel weight is given by,

$$(\Delta W_f)_i = [T_{SL}\sigma_i]\,(c_T)_i \Delta t_i \tag{39}$$

This resulted in the following conclusions,

$$T_c = 11.57 \ \ minutes \tag{40}$$

$$F_c = 5502.62 \ \ N \tag{41}$$

Where T_c is the Time to climb, and F_c is the Fuel to climb.

4.16 Inferences

The Rate of Climb for various altitudes were plotted, and the best rate of climb and the best climb speed were obtained. Further, the variation of thrust and TSFC with altitude were plotted. The thrust has an exponential relation with altitude, whereas the TSFC varies linearly till 11 km, after which it is constant. These results conform to the general trend of the ISA model. Further, the time of climb was also calculated and was found to have decreased with a decrease in take-off weight (W_{TO}).

5 Turn Performance

5.1 Preliminary Calculations

The turn performance was analysed for steady, coordinated turning flight. The main factors affecting turn performance are the turn rate (ω), the radius of turn (R) and the load factor (n). The stall, structural and propulsive boundaries lift the turn capabilities of the aircraft. Two quantities that need elucidation are the sustained and attained turn rates, represented by STR and ATR, respectively.

The attained turn rate (ATR) corresponds to the turn rate at the corner speed. In contrast, the maximum sustained turn rate (STR) corresponds to the maximum turn rate on the propulsive boundary. The turn performance analyses were carried at two weights, namely 0.8 W_{TO} and 0.9 W_{TO}. These were carried out at two altitudes of 0.5 Km and 5 Km, respectively. The turn rate (ω) is given by,

$$\omega = \frac{g\sqrt{n^2 - 1}}{V} \tag{42}$$

Where n is the load factor and is given by,

$$n = \frac{L}{W} \tag{43}$$

It is also given by,

$$n = \sqrt{\left[\frac{\frac{1}{2}\rho_\infty V_\infty^2}{K\,(W/S)}\left(\frac{T}{W} - \frac{1}{2}\rho_\infty V_\infty^2 \frac{C_{D_0}}{W/S}\right)\right]} \tag{44}$$

The turn rate is also given by,

$$\omega = \frac{V}{R} \tag{45}$$

The stall boundary is given by,

$$V_{stall} = \sqrt{\frac{2nW}{\rho S C_{L_{max}}}} \tag{46}$$

The sustained turn rate boundary is given by,

$$AV^4 - TV^2 + Bn^2 = 0 \tag{47}$$

where A = ${}^{C_{D_0}\rho S}/_{2}$ and B = ${}^{2kW^2}/_{\rho S}$. The bank angle boundary (ϕ_{max}) was plotted using the relation,

$$\phi = tan^{-1}(\sqrt{n^2 - 1}) \tag{48}$$

The maximum load factor (structural limit), according to the constraints of the problem, was assigned a value of 2.5 (n_{max}).

5.2 Turn Performance for 0.9 W_{TO} and Altitude 0.5 Km

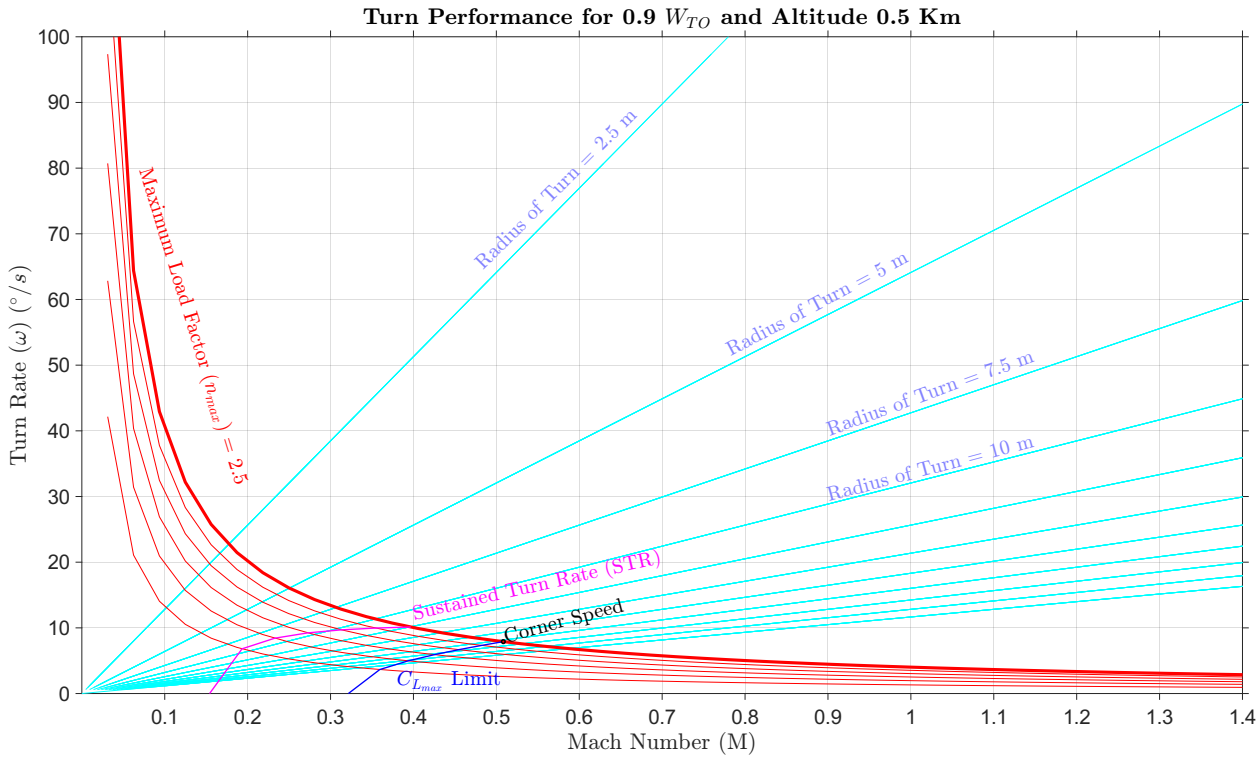

5.3 Turn Performance for 0.9 W_{TO} and Altitude 5 Km

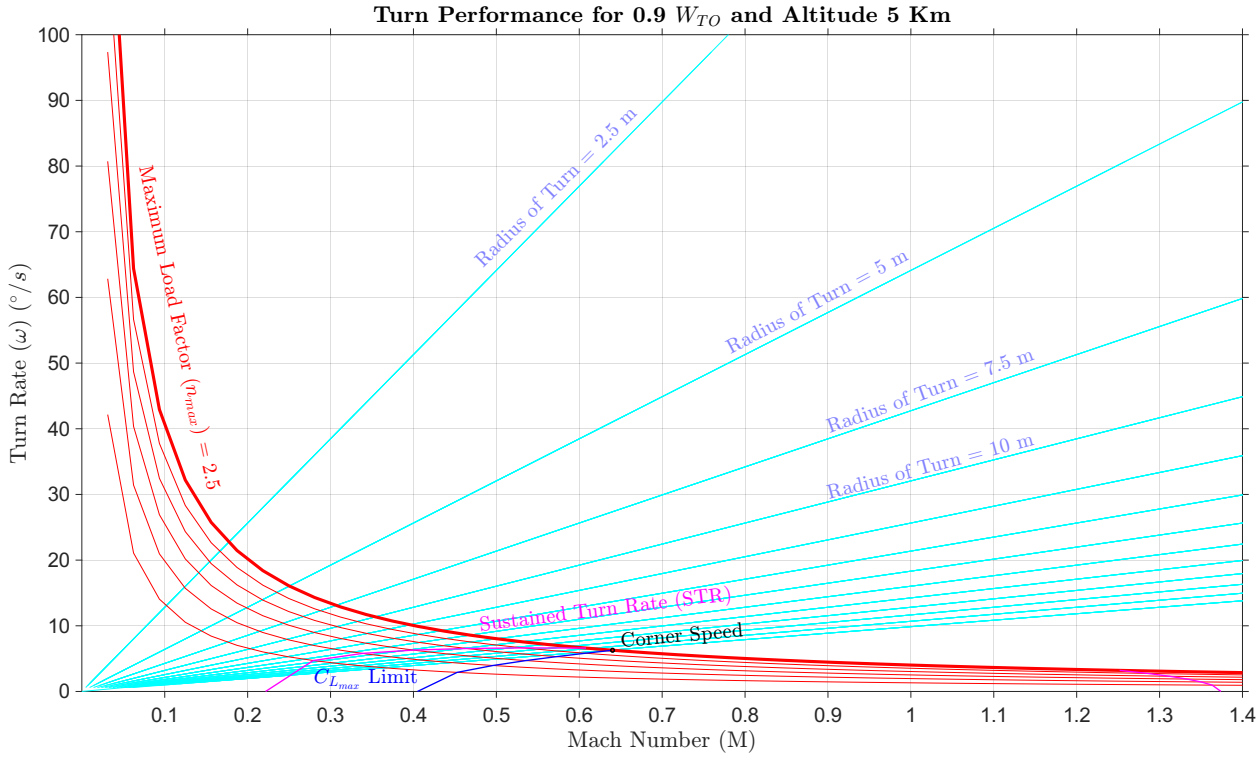

5.4 Turn Performance for 0.8 W_{TO} and Altitude 0.5 Km

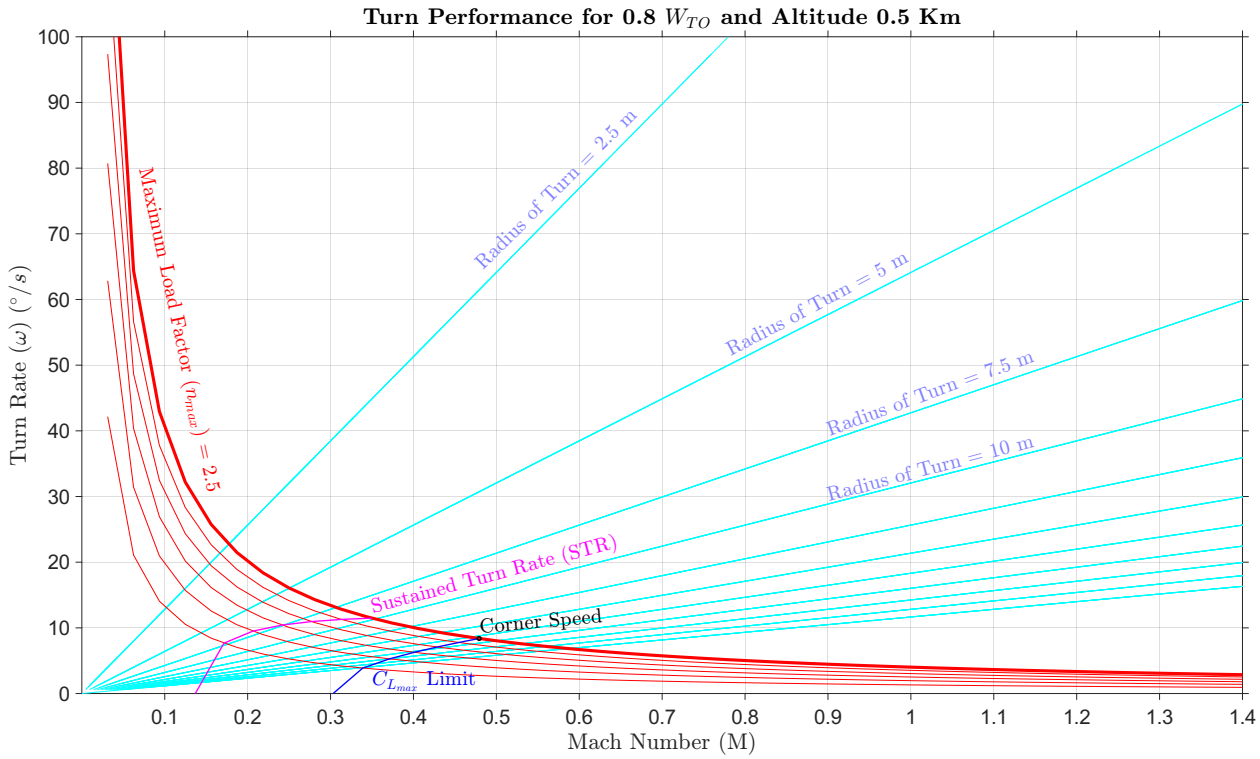

5.5 Turn Performance for 0.8 W_{TO} and Altitude 5 Km

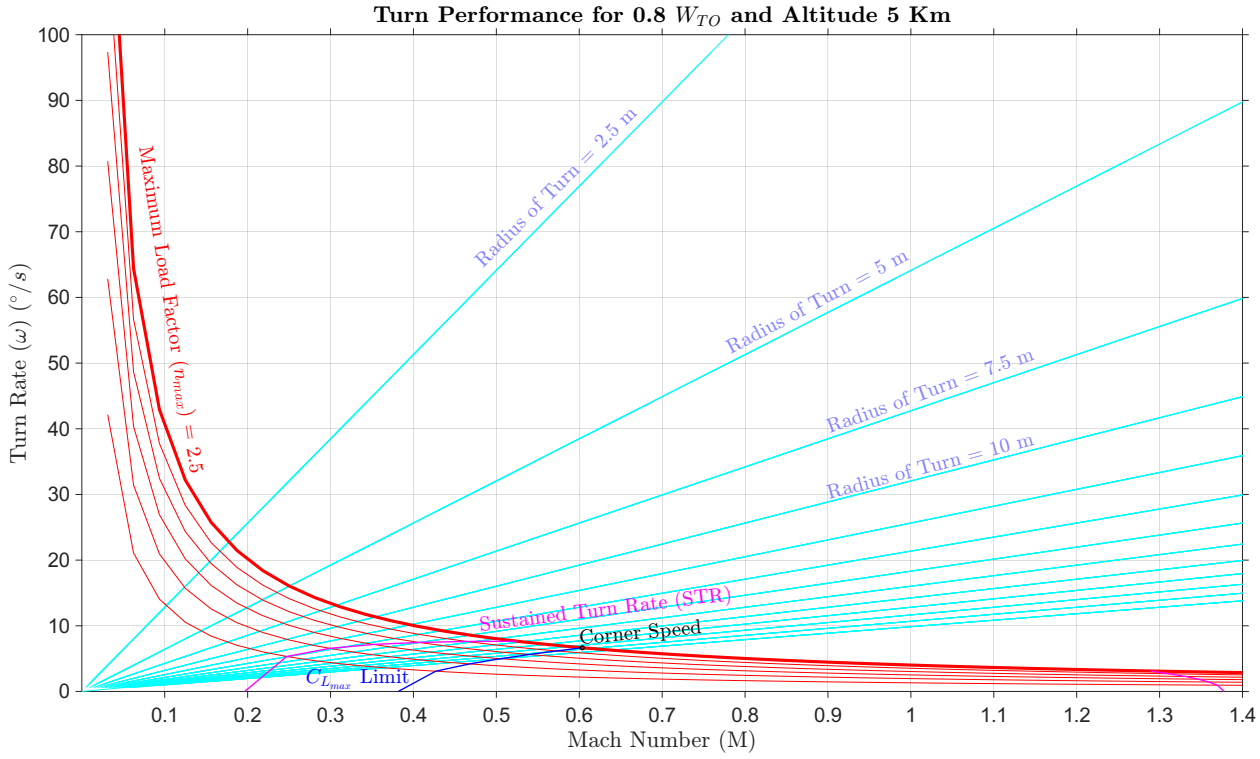

5.6 Turn Performance for 0.9 W_{TO} and Altitude 0.5 Km

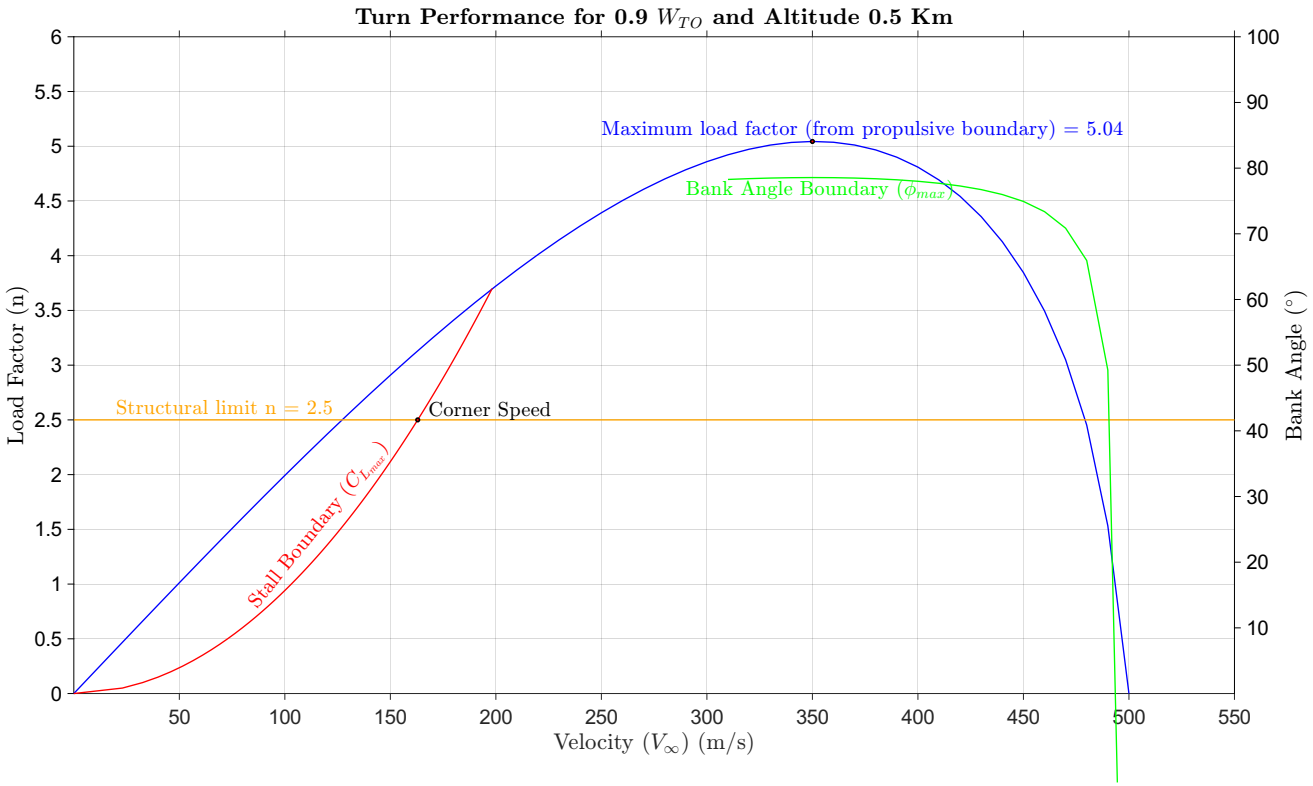

5.7 Turn Performance for 0.9 W_{TO} and Altitude 5 Km

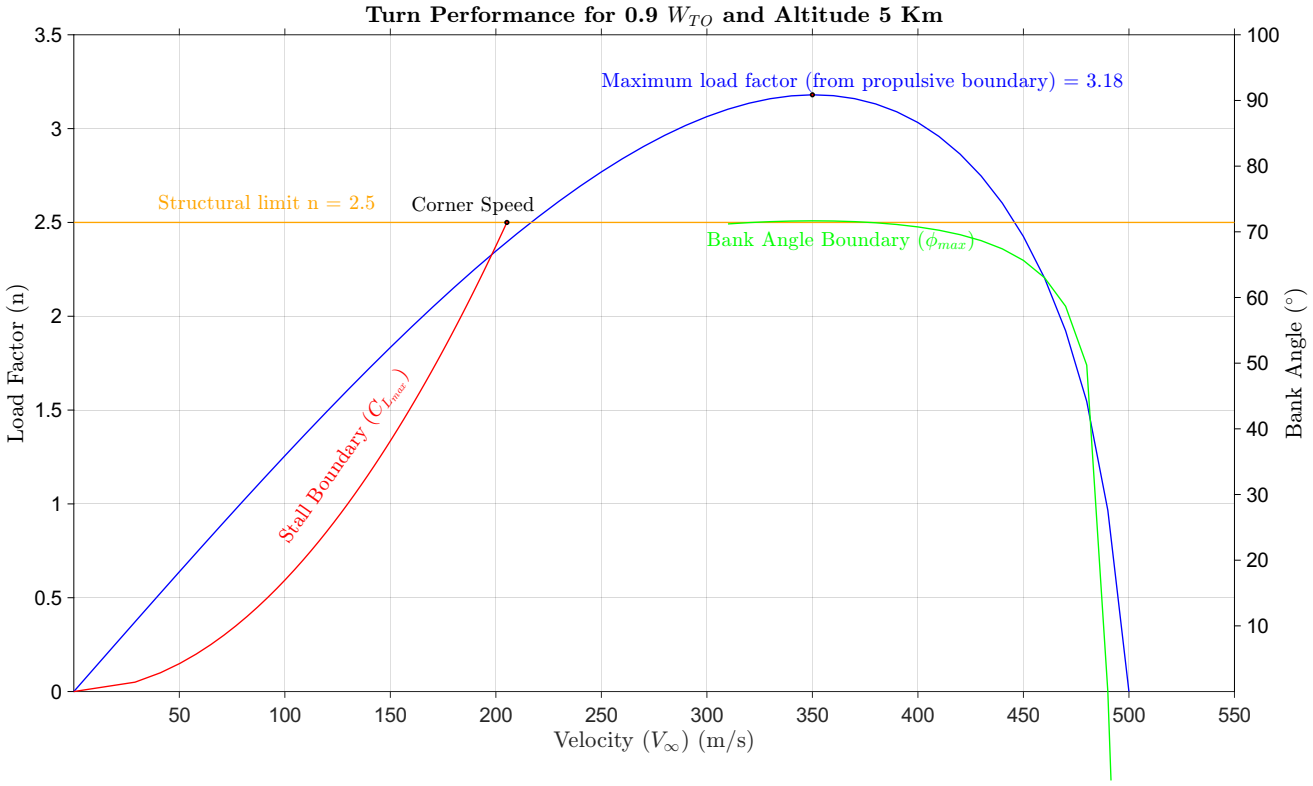

5.8 Turn Performance for 0.8 W_{TO} and Altitude 0.5 Km

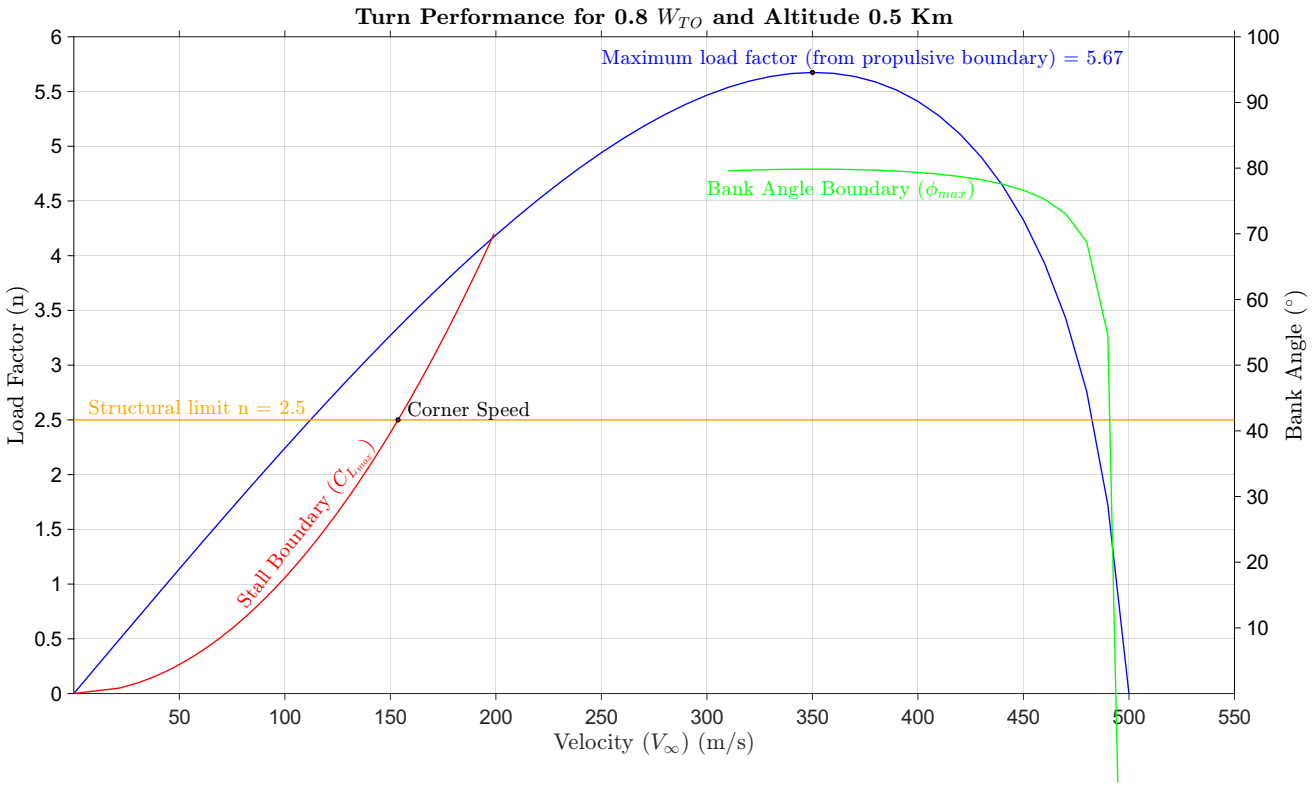

5.9 Turn Performance for 0.8 W_{TO} and Altitude 5 Km

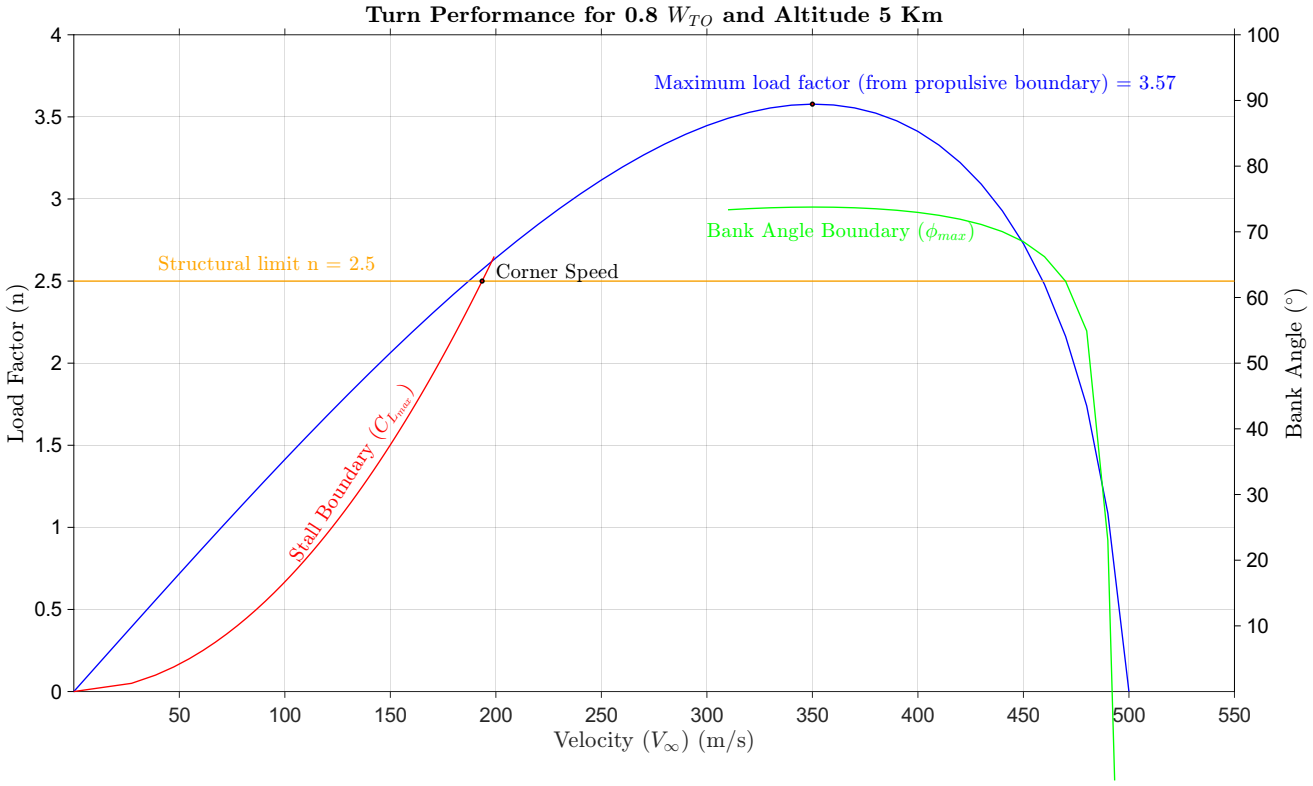

5.10 Turn Performance for 0.9 W_{TO} and Altitudes 0.5 and 5 Km

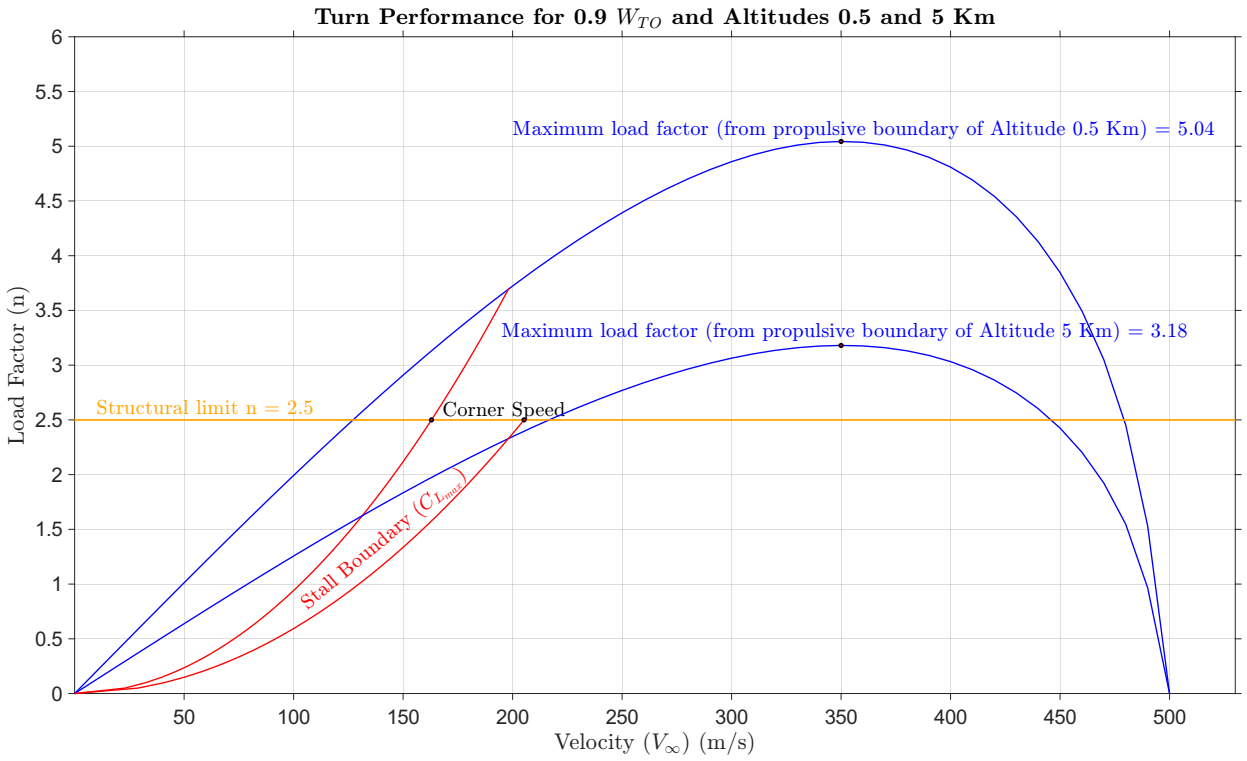

5.11 Turn Performance for 0.8 W_{TO} and Altitudes 0.5 and 5 Km

5.12 Turn Performance Characteristics

Parameter	Value
n_{max}	2.5
Corner Speed	Mach 0.51
ATR	7.90 $^\circ/s$
STR	10.13 $^\circ/s$

Parameter	Value
n_{max}	2.5
Corner Speed	Mach 0.64
ATR	6.28 $^\circ/s$
STR	6.61 $^\circ/s$

Table 15: Data for 0.9 W_{TO} corresponding to 0.5 km and 5 km (left to right)

Parameter	Value
n_{max}	2.5
Corner Speed	Mach 0.48
ATR	8.38 $^\circ/s$
STR	11.71 $^\circ/s$

Parameter	Value
n_{max}	2.5
Corner Speed	Mach 0.60
ATR	6.66 $^\circ/s$
STR	7.58 $^\circ/s$

Table 16: Data for 0.8 W_{TO} corresponding to 0.5 km and 5 km (left to right)

5.13 Inferences

The turn performance polars (ω versus V and n versus V) were plotted for ranging values of take-off weights W_{TO} and altitudes. The attained turn rate corresponds to the turn rate at the corner speed in all the above polars. The maximum load factor from the propulsive boundary was found to decrease with an increase in altitude. The aircraft's turn performance was analysed, and the operational limits were determined.

6 Take Off Performance

6.1 Preliminary calculations

The aircraft's take-off performance was analysed using the iterative method described in reference [6]. The performance was analysed at $0.9W_{TO}$ and $0.8W_{TO}$ at a take-off altitude of 0.5 km. It was assumed that partial flaps are deflected during take-off, and the suitable constraints were applied. The time step integrated Pamadi's method is as follows,

$$\Delta t = 0.25\ s \tag{49}$$

$$q_i S = \frac{1}{2}\rho V_i^2 S \tag{50}$$

Thus lift and drag can be calculated,

$$L_i = C_L q_i S \tag{51}$$

$$D_i = C_D q_i S \tag{52}$$

Hence acceleration can be calculated,

$$a_i = \frac{[T - D - \mu(W - L_i)] \times g}{W} \tag{53}$$

The change in velocity is given by,

$$\Delta V_i = a_i \Delta t \tag{54}$$

The change in distance is given by,

$$\Delta s_i = V_i \, \Delta t + \frac{1}{2} a_i \, \Delta t^2 \tag{55}$$

The velocity at the end of each iteration is given by,

$$V_{i+1} = V_i + \Delta V_i \tag{56}$$

Similarly, the distance at the end of each iteration is given by,

$$s_{i+1} = s_i + \Delta s_i \tag{57}$$

Similarly, the time at the end of each iteration is given by,

$$t_{i+1} = t_i + \Delta t_i \tag{58}$$

This is used to calculate the ground acceleration distance. The rotation distance for 3 seconds is given by,

$$s_{rot} = 3 \times V_{rot} \tag{59}$$

where,

$$V_{rot} = 1.2 \times V_{stall} \tag{60}$$

The distance to climb is given by,

$$s_{climb} = \frac{10.7}{\tan \gamma} \tag{61}$$

where,

$$\sin \gamma = \frac{T - D}{W} \tag{62}$$

The time to climb is given by,

$$t_{climb} = \frac{10.7}{V_{rot} \tan \gamma} \tag{63}$$

Therefore the total time and distance for take-off are given by,

$$t = t_{gr\,accn} + t_{rot} + t_{climb} \tag{64}$$

$$s = s_{gr\,accn} + s_{rot} + s_{climb} \tag{65}$$

The take-off distance for a multi-engine aircraft as per the Federal Aviation Regulations (FAR) is taken as the higher of the two following distances,

* 115% of the distance required to clear 35 ft (10.7 m) obstruction with all engines operating (AEO).

* Balanced Field Length with one engine inoperative (OEI) (to be estimated for the failure of most critical of the engines).

6.2 Take-Off Characteristics for All Engines Operating (AEO)

Parameter	Value
Take-off Time	48.82 s
Take-off Distance	2,316.51 m

Parameter	Value
Take-off Time	41.04 s
Take-off Distance	1,898.68 m

Table 17: Data for 0.9 W_{TO} corresponding to 0.5 km and 1.5 km (left to right)

Parameter	Value
Take-off Time	41.03 s
Take-off Distance	1,858.59 m

Table 18: Data for 0.8 W_{TO} corresponding to 0.5 km

6.3 Take-Off Characteristics for One Engine Inoperative (OEI)

6.3.1 Accelerate Stop Distance Required (ASDR)

Velocity	ASDR	Time
0.65 V_R	1,663.4 m	55.25 s
0.70 V_R	2,000.8 m	61.00 s
0.75 V_R	2,256.2 m	65.50 s
0.80 V_R	2,480.3 m	69.50 s
0.85 V_R	2,698.8 m	73.50 s
0.90 V_R	2,911.6 m	77.50 s
0.95 V_R	3,118.5 m	81.50 s
V_R	3,341.4 m	85.75 s

Velocity	ASDR	Time
0.65 V_R	1,931.9 m	61.50 s
0.70 V_R	2,312.0 m	67.75 s
0.75 V_R	2,586.5 m	72.25 s
0.80 V_R	2,827.2 m	76.50 s
0.85 V_R	3,081.9 m	81.25 s
0.90 V_R	3,326.0 m	85.75 s
0.95 V_R	3,559.2 m	90.50 s
V_R	3,781.4 m	95.00 s

Table 19: Data for 0.9 W_{TO} corresponding to 0.5 km and 1.5 km (left to right)
Where $V_{R_{0.5\,km}} = 87.45$ m/s and $V_{R_{1.5\,km}} = 91.86$ m/s.

6.3.2 Take-Off Distance Required (TODR)

Velocity	TODR	Time
0.65 V_R	2,454.1 m	51.50 s
0.70 V_R	2,414.3 m	50.75 s
0.75 V_R	2,365.4 m	50.00 s
0.80 V_R	2,297.3 m	49.00 s
0.85 V_R	2,247.2 m	48.25 s
0.90 V_R	2,170.9 m	47.25 s
0.95 V_R	2,090.3 m	46.25 s
V_R	2,005.0 m	45.25 s

Velocity	TODR	Time
0.65 V_R	3,053.6 m	60.75 s
0.70 V_R	2,991.2 m	59.75 s
0.75 V_R	2,925.3 m	58.75 s
0.80 V_R	2,837.2 m	57.50 s
0.85 V_R	2,762.3 m	56.50 s
0.90 V_R	2,660.2 m	55.25 s
0.95 V_R	2,576.4 m	54.25 s
V_R	2,464.8 m	53.00 s

Table 20: Data for 0.9 W_{TO} corresponding to 0.5 km and 1.5 km (left to right)
Where $V_{R_{0.5\,km}} = 87.45$ m/s and $V_{R_{1.5\,km}} = 91.86$ m/s.

6.4 Balanced Field Length for a Take-Off Altitude of 0.5 km and 0.9 W_{TO}

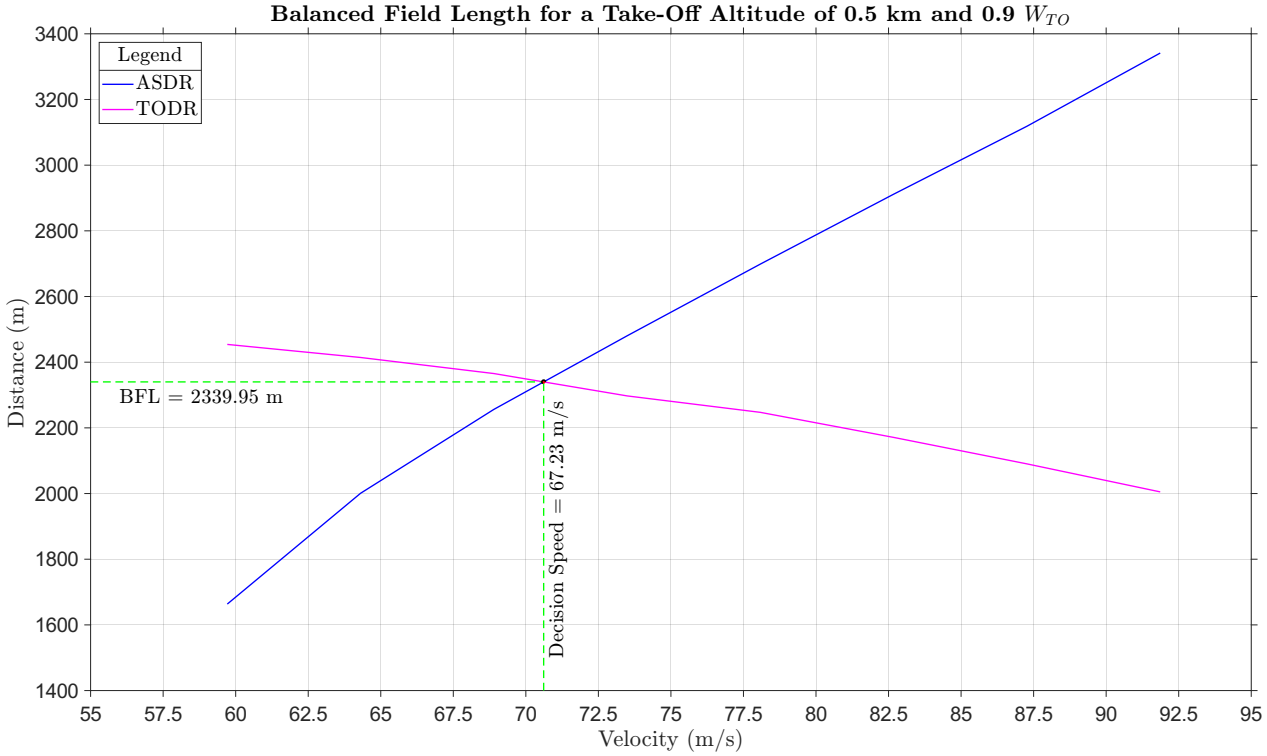

6.5 Balanced Field Length for a Take-Off Altitude of 1.5 km and 0.9 W_{TO}

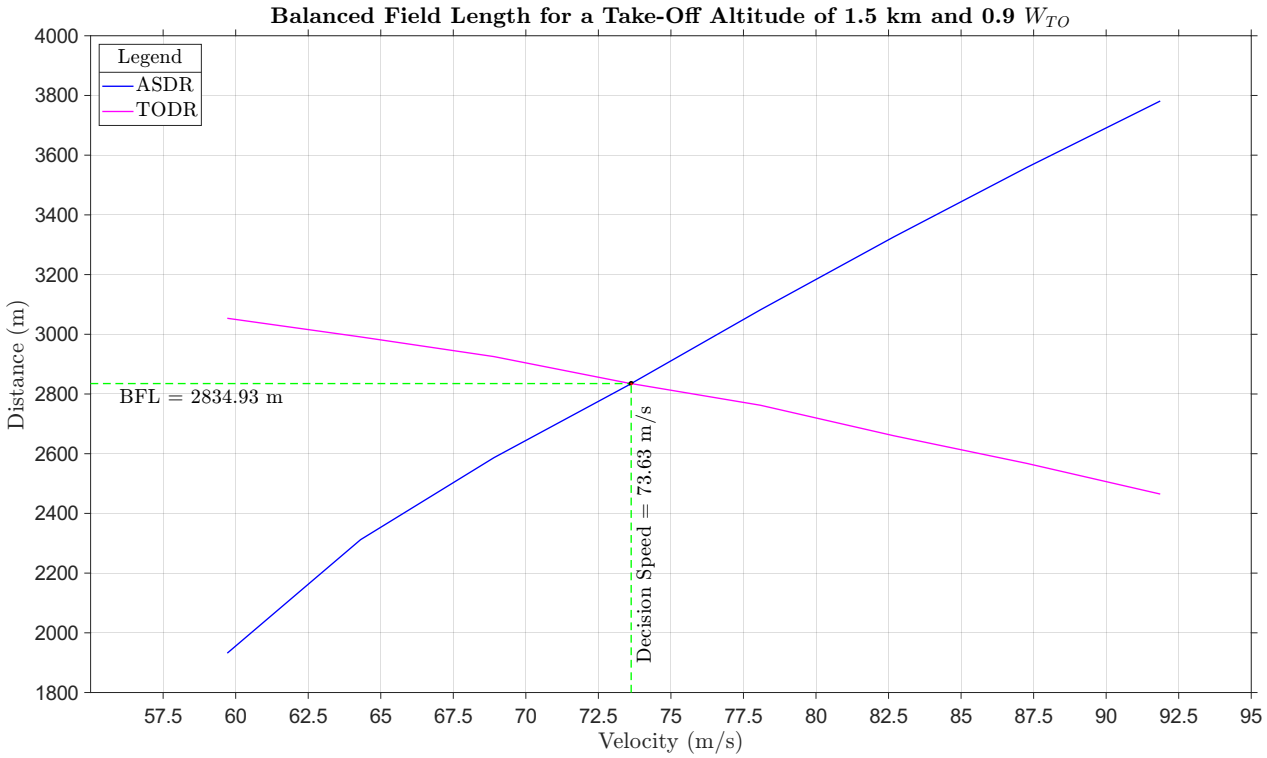

6.6 Take-Off Distance from FAR

Take off distance calculated using FAR for 0.5 km and 0.9 W_{TO} is,

$$s = 2,663.98\, m$$

Take off distance calculated using FAR for 1.5 km and 0.9 W_{TO} is,

$$s = 2,834.93\, m$$

6.7 Inferences

The take-off distance for AEO at 0.5 km for 0.9 W_{TO} and 0.8 W_{TO} was calculated. Further, the take-off distance for AEO at 1.5 km for 0.9 W_{TO} was also calculated. A scenario of one engine failure (OEI) was analysed at different failure speeds, and the respective ASDR and TODR were calculated. This was done for 1.5 km and 0.9 W_{TO}. It was observed that ASDR increases with velocity while the TODR decreases withand increase in velocity. It was also observed that the take-off distance for the same take-off weight (W_{TO}) decreases with an increase in altitude. Conversely, the ASDR and TODR increased with altitude for the same take-off weight (W_{TO}).

7 Landing Performance

7.1 Preliminary Calculations

The modified Pamadi's approach was used to calculate the landing distance (see reference [7]). Since the take-off performance analyses were conducted at 0.5 km, this value was retained for the landing performance analyses for the sake of consistency. The deceleration levels were limited to 0.25g. The obstacle height is considered to be 50 ft. The approach distance is given by,

$$s_a = \frac{15.2}{\tan \gamma_a} \tag{66}$$

where,

$$\gamma_a = \sin^{-1}\left(\frac{C_D/C_{L_{max}}}{T/W}\right) \tag{67}$$

γ_a is in radians. For a civil transport aircraft, γ_a is 3°. The approach speed is given by,

$$V_a = 1.3 \times V_{stall} \tag{68}$$

The flare distance is given by,

$$s_f = 0.1248 \times V_{stall}^2 \times \gamma_f \tag{69}$$

where,

$$\gamma_f = \gamma_a \tag{70}$$

The rotation distance is given by,

$$s_r = 3 \times V_a \tag{71}$$

The braking distance is given by,

$$s_b = \frac{V_a^2}{2a} \tag{72}$$

Hence the landing distance is given by,

$$s = s_a + s_f + s_r + s_b \tag{73}$$

7.2 Landing Distance

The landing distance calculated using modified Pamadi's method at 0.5 km and 0.8 W_{TO}

$$s = 1771.73\,m$$

The landing distance calculated using modified Pamadi's method at 0.5 km and 0.6 W_{TO}

$$s = 1428.53\,m$$

7.3 Inferences

The landing distance was calculated using the modified Pamadi's method. It was observed that with a decrease in the weight of the aircraft, the landing distance was reduced.

8 Payload v/s Range Trade-Off

8.1 Preliminary Calculations

The methodology used corresponds to the methodology elucidated in reference [9]. The total fuel capacity was considered to be 130% of the fuel weight (W_{fuel}). The fuel burnt to reach the cruise altitude was assumed to be 5% of the fuel weight. The weight at the end of the cruise was assumed to be 7% of the fuel weight. Thus the following relations were derived,

$$W_A = W_{TO} - 0.05\,W_{Fuel} \tag{74}$$

$$W_B = W_{TO} - 0.93\,W_{Fuel} \tag{75}$$

$$W_E = W_{TO} - 0.05\,W_{Fuel} \tag{76}$$

$$W_C = W_{TO} - 1.23\,W_{Fuel} \tag{77}$$

$$W_F = W_{TO} - (1/3)(W_{PL})_E - 0.05\,W_{Fuel} \tag{78}$$

$$W_G = W_{TO} - (1/3)(W_{PL})_E - 1.23\,W_{Fuel} \tag{79}$$

$$W_H = W_{TO} - (2/3)(W_{PL})_E - 0.05\,W_{Fuel} \tag{80}$$

$$W_I = W_{TO} - (2/3)(W_{PL})_E - 1.23\,W_{Fuel} \tag{81}$$

$$W_O = W_{TO} - (W_{PL})_E - 0.05\,W_{Fuel} \tag{82}$$

$$W_O = W_{TO} - (W_{PL})_E - 1.23\,W_{Fuel} \tag{83}$$

The range equation of a turbofan engine-powered aircraft is given by,

$$R = \frac{2}{c_t}\sqrt{\frac{2}{\rho_\infty S}}\frac{C_L^{1/2}}{C_D}\left(\sqrt{W_0} - \sqrt{W_1}\right) \tag{84}$$

The speed for maximum range cruise corresponds to $(D/V)_{min}$ and is quantified as,

$$V_{R_{max}} = V_{(C_L^{1/2}/C_D)_{max}} = \sqrt{\frac{2}{\rho_\infty}\frac{W}{S}\sqrt{\frac{3k}{C_{D_0}}}} \tag{85}$$

$C_{L_{opt}}$ (C_L for $(L/D)_{max}$) is given by,

$$C_{L_{opt}} = \sqrt{\frac{C_{D_0}}{k}} \tag{86}$$

Thus $V_{R_{max}}$ can be written as,

$$V_{R_{max}} = V_{(C_L^{1/2}/C_D)_{max}} = \sqrt{\frac{2}{\rho_\infty}\frac{W}{S}\frac{\sqrt{3}}{C_{L_{opt}}}} \tag{87}$$

$(C_L^{1/2}/C_D)_{max}$ is also given by,

$$\left(\frac{C_L^{1/2}}{C_D}\right)_{max} = \frac{3}{4}\left(\frac{1}{3kC_{D_0}^3}\right)^{\frac{1}{4}} \tag{88}$$

Hence the range for a jet aircraft can be written as,

$$R = \frac{2}{c_t}\sqrt{\frac{2}{\rho_\infty S}}\frac{3}{4}\left(\frac{1}{3kC_{D_0}^3}\right)^{\frac{1}{4}}\left(\sqrt{W_0} - \sqrt{W_1}\right) \tag{89}$$

The Breguet Range is given by,

$$R = \frac{V_\infty}{c_t}\frac{L}{D}\ln\frac{W_0}{W_1} \tag{90}$$

C_D for $(L/D)_{max}$ is given by,

$$C_D = 2C_{D_0} \tag{91}$$

Thus $(L/D)_{max}$ is given by,

$$\left(\frac{L}{D}\right)_{max} = \frac{1}{2\sqrt{C_{D_0}k}} \tag{92}$$

The following results were obtained,

$$V_{R_{max}} = 314.19\, m/s \tag{93}$$

$$V_{crit} = 264.09\, m/s \tag{94}$$

From the above relations, it is observed that the velocity for the maximum range exceeds the critical velocity. Hence the critical velocity was taken for all the range calculations.

8.2 Payload v/s Range Diagram for a Cruise Altitude of 12 km

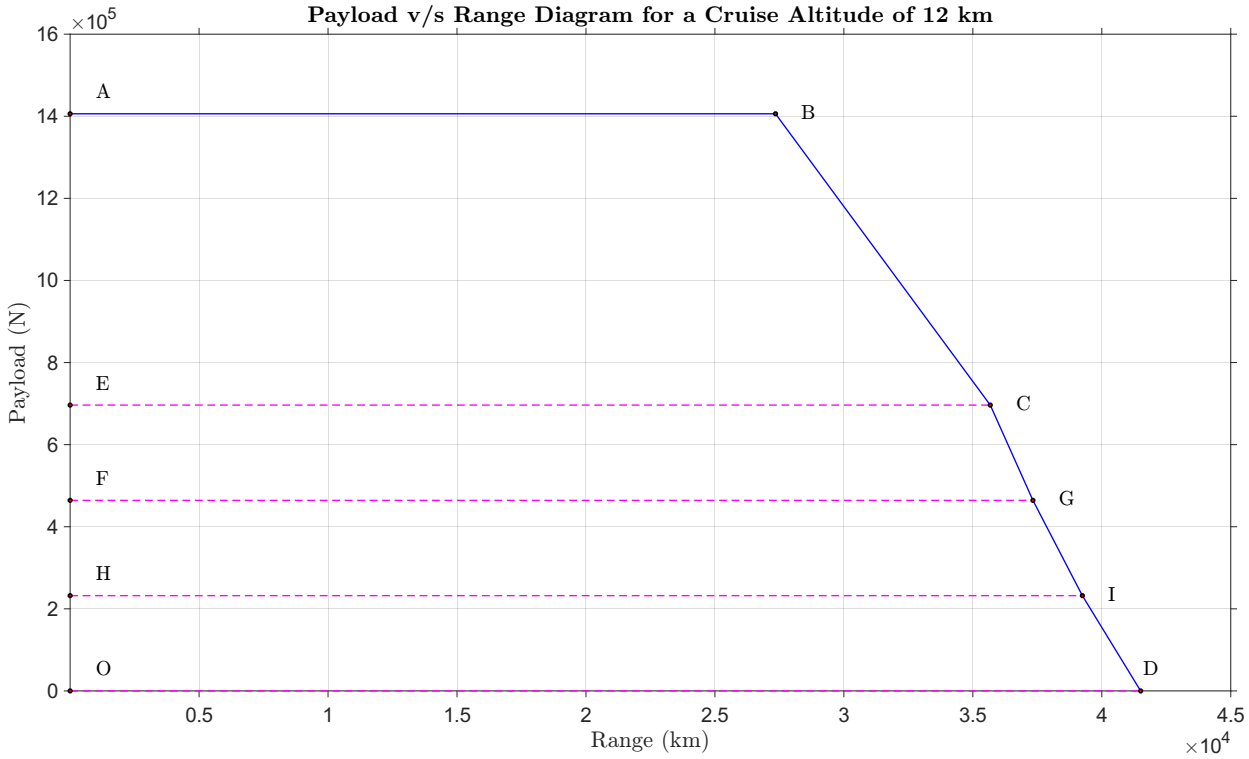

8.3 Payload v/s Breguet Range Diagram for a Cruise Altitude of 12 km

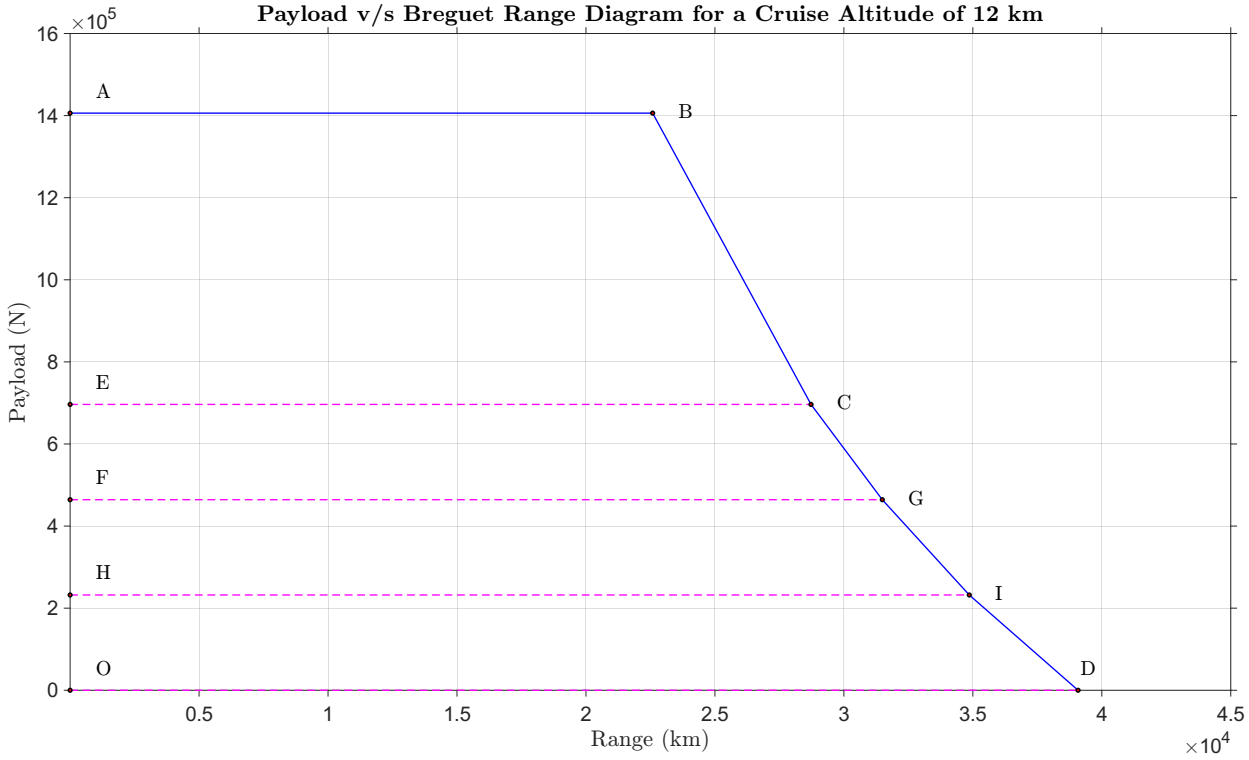

8.4 Combined Payload v/s Range Diagram for a Cruise Altitude of 12 km

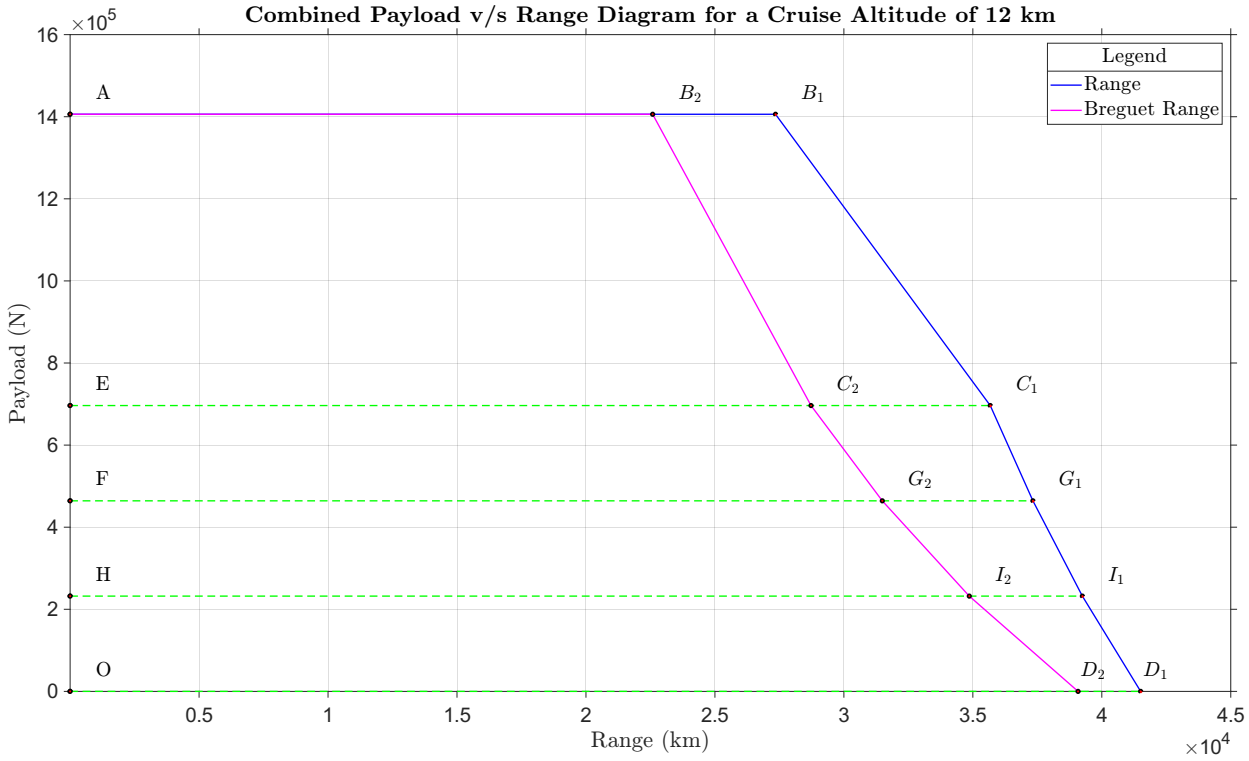

8.5 Key Findings

The following parameters were used,

$$W_{OE} = 2725\ kN \tag{95}$$

$$W_{PL} = 1406\ kN \tag{96}$$

$$W_{Fuel} = 2365.5\ kN \tag{97}$$

$$W_{TO} = 6496.5\ kN \tag{98}$$

$$S = 845\ m^2 \tag{99}$$

For maximum range,

$$C_{L_{R\,max}} = 0.2893 \tag{100}$$

$$\left(\frac{C_L^{1/2}}{C_D}\right)_{max} = 36.6736 \tag{101}$$

The TSFC is given by,

$$c_{t_{SL}} = 1.2943e^{-04} \tag{102}$$

$$c_{t_{12\,km}} = 1.1224e^{-04} \tag{103}$$

The ferry range of the aircraft was calculated to be 41506.45 km. The design range of the aircraft is 14800 km. However, upon calculation it was found that the range of segment AB, the segment corresponding to the design range, was 27349.11 km. This difference in the ranges could be caused due to several factors.

The W_{TO} considered only 95% of the payload and the fuel weights. Further provisions were given for loiter time, two climbs and diversions taking into the safety aspects of the aircraft. Further, the engine performance data assumed could vary in contrast to actual engine data. The following equation is derived from the basic thermodynamic principles of jet engine operation, and it assumes that the engine is operating at its maximum efficiency. This was used to determine engine TSFC at an altitude (θ can be determined from ISA).

$$c_T = 49.5\sqrt{\theta} \tag{104}$$

The study conducted above showed that the Breguet range (assuming constant speed) was lower when compared to the range achieved from the constant altitude/C_L approach (range for jet aircraft). Considering the piloting technique, constant speed flight would be less intensive and fuel inefficient. Constant altitude flight, on the other hand, would need continuous velocity adjustment due to the decreasing aircraft weight over time and would be more intensive. That being said, this technique of flying would be fuel efficient, and the maximum range can be achieved.

9 Conclusion

The performance analysis on the assigned aircraft, the Airbus A380 800M, was conducted. The drag polar, the flight envelope and the rate of climb polar were generated. The turn, take-off and landing performances were analysed. In the take-off performance, several scenarios were considered, including the AEO and OEI at several failure speeds, and meaningful conclusions were drawn. Finally, a payload versus range trade-off study was conducted. Suitable inferences were drawn along the way, which led to significant results. This concludes a comprehensive study conducted on seven aspects of the aircraft characteristics.

10 References

* Dr. Tonse Gokuldas Pai, "AAE 2256 Flight Mechanics Scope of Group Projects & Annexure on Aircraft Data 31 Jan 2023", *Manipal Institute of Technology - FM, 2022-23*
* Dr. Tonse Gokuldas Pai, "AAE 2256 Ch 05 Level Flight and Aircraft Flight Envelope", *Manipal Institute of Technology - FM, 2022-23*
* Dr. Tonse Gokuldas Pai, "AAE 2256 Ch 03 Review of Aerodynamics", *Manipal Institute of Technology - FM, 2022-23*
* Dr. Tonse Gokuldas Pai, "AAE 2256 Ch 06 Climb Performance", *Manipal Institute of Technology - FM, 2022-23*
* Dr. Tonse Gokuldas Pai, "AAE 2256 Ch 08 Turn Performance", *Manipal Institute of Technology - FM, 2022-23*
* Dr. Tonse Gokuldas Pai, "AAE 2256 Ch 10 Take Off Peformance and Balanced Field Length", *Manipal Institute of Technology - FM, 2022-23*
* Dr. Tonse Gokuldas Pai, "AAE 2256 Ch 11 Landing Peformance", *Manipal Institute of Technology - FM, 2022-23*

* Dr. Tonse Gokuldas Pai, "AAE 2256 Ch 12 Range & Endurance", *Manipal Institute of Technology - FM, 2022-23*

* Dr. Tonse Gokuldas Pai, "AAE 2256 Trade off between Range and Pay Load Gp Proj Q 6", *Manipal Institute of Technology - FM, 2022-23*

11 Appendix

11.1 List of Tables

11.2 List of Figures

Figure	Description	Figure	Description
7	Drag Polar for 5.5 km	30	Variation of R/C with Altitude for 0.9 W_{TO}
8	Drag Polar for 8.5 km	31	Turn Performance for 0.9 W_{TO} and Altitude 0.5 Km
9	Drag Polar for 10.5 km	32	Turn Performance for 0.9 W_{TO} and Altitude 5 Km
10	Drag Polar for 11.5 km	33	Turn Performance for 0.8 W_{TO} and Altitude 0.5 Km
11	V-h Plot for 0.9 W_{TO} and 100% Throttle	34	Turn Performance for 0.8 W_{TO} and Altitude 5 Km
12	V-h Plot for 0.8 W_{TO} and 100% Throttle	35	Turn Performance for 0.9 W_{TO} and Altitude 0.5 Km
13	V-h Plot for 0.6 W_{TO} and 100% Throttle	36	Turn Performance for 0.9 W_{TO} and Altitude 5 Km
14	V-h Plot for 0.9 W_{TO} and 95% Throttle	37	Turn Performance for 0.8 W_{TO} and Altitude 0.5 Km
15	V-h Plot for 0.9 W_{TO} and 82.5% Throttle	38	Turn Performance for 0.8 W_{TO} and Altitude 5 Km
16	V-h Plot for 0.9 W_{TO} and 70% Throttle	39	Turn Performance for 0.9 W_{TO} and Altitudes 0.5 and 5 Km
17	Combined V-h Plot for 0.9 W_{TO}	40	Turn Performance for 0.8 W_{TO} and Altitudes 0.5 and 5 Km
18	Rate Of Climb Plot for 0.9 W_{TO}	41	Balanced Field Length for a Take-Off Altitude of 0.5 km and 0.9 W_{TO}
19	Rate Of Climb Plot for 0.8 W_{TO}	42	Balanced Field Length for a Take-Off Altitude of 1.5 km and 0.9 W_{TO}
20	$(R/C)_{max}$ for 0.9 W_{TO}	43	Payload v/s Range Diagram for a Cruise Altitude of 12 km
21	$(R/C)_{max}$ for 0.8 W_{TO}	44	Payload v/s Breguet Range Diagram for a Cruise Altitude of 12 km
22	h v/s $(R/C)_{max}$ for 0.9 W_{TO}	45	Combined Payload v/s Range Diagram for a Cruise Altitude of 12 km
23	h v/s $(R/C)_{max}$ for 0.8 W_{TO}		

11.3 List of Symbols and Abbreviations

Symbol	Description	Symbol	Description
FM	Flight Mechanics	S	Planform Area
AR	Aspect Ratio	q_∞	Dynamic Pressure
V_∞	Freestream Velocity	M_{crit}	Critical Mach Number
V_{stall}	Stall Velocity	V_{crit}	Critical Velocity
h	Altitude	C_L	Coefficient of Lift
C_D	Coefficient of Drag	C_{D_i}	Coefficient of Induced Drag
C_{D_0}	Coefficient of Parasitic Drag	e	Oswald's Efficiency Factor
TSFC	Thrust Specific Fuel Consumption	$C_{L_{max}}$	Maximum Coefficient of Lift
$V_{D_{min}}$	Velocity at Minimum Drag	D_{min}	Minimum Drag
W_{TO}	Take-off Weight	ρ	Density
σ	Density Ratio	θ	Temperature Ratio
h_{abs}	Absolute Ceiling	P_{avb}	Power Available
P_{reqd}	Power Required	R/C	Rate of Climb
$(R/C)_{max}$	Maximum Rate of Climb	ω	Turn rate
n_{max}	Maximum Load Factor (n)	ϕ	Bank Angle
n	Load Factor	R	Radius of Turn
W/S	Wing Loading	T/W	Thrust to Weight Ratio
g	Acceleration Due to Gravity	ISA	International Standard Atmosphere
STR	Sustained Turn Rate	ATR	Attained Turn Rate
c_T	TSFC of a turbofan aircraft	BFL	Balanced Field Length
ASDR	Accelerate Stop Distance Required	TODR	Take-Off Distance Required
μ	Coefficient of Rolliing Friction	ΔV	Incremental Velocity
Δt	Incremental Time	Δs	Incremental Distance
γ	Climb Angle	FAR	Federal Aviation Regulations
AEO	All Engines Operational	OEI	One Engine Inoperative
$V_{R_{max}}$	Velocity for Maximum Range	V_R	Rotation Velocity
HLD	High Lift Devices	W_{TO}	Take-Off Weight
$V_{R_{max}}$	Velocity for Maximum Range	W_{OE}	Operational Empty Weight
W_{Fuel}	Fuel Weight	W_{PL}	Payload Weight